MODELING ATMOSPHERIC DISPERSION OF LEAD PARTICULATES FROM A HIGHWAY

by
Paul C. Katen

1870

Environmental Research Papers
COLORADO STATE UNIVERSITY
Fort Collins, Colorado

11

Research on the environment constitutes an important component of the graduate programs pursued by a number of Colorado State University departments. The more noteworthy results of these research efforts are normally published in the conventional professional journals or conference proceedings, but in very much abridged form. ENVIRONMENTAL RESEARCH PAPERS has been established to provide a formal means of disseminating such CSU accomplishments in all significant details, in order that individuals concerned with related interests at other institutions may review a more comprehensive treatment of the research reported than is customarily available.

Price $3.00 in USA

Subscriptions and correspondence to these papers should be addressed to: Secretary of Environmental Research Papers, Department of Atmospheric Science, Colorado State University, Solar Village, Ft. Collins, CO 80523.

MODELING ATMOSPHERIC DISPERSION OF LEAD PARTICULATES FROM A HIGHWAY

By

PAUL C. KATEN

ENVIRONMENTAL RESEARCH PAPERS
COLORADO STATE UNIVERSITY
FORT COLLINS, COLORADO

OCTOBER 1977 No. 11

From a dissertation submitted to the Graduate Faculty of Colorado State University in partial fulfillment of the requirements for the degree of Doctor of Philosophy.

TABLE OF CONTENTS

LIST OF TABLES

LIST OF FIGURES

LIST OF SYMBOLS

A, B	Scaling lengths
c	Concentration
g	Acceleration due to gravity
h	Source height
I	Bessel function
k	von Karmon constant
K	Eddy diffusivity of pollutant
K_m	Eddy diffusivity for momentum
K_v	Eddy diffusivity attributable to vehicular traffic
K_H	Eddy diffusivity for heat
K_w	Eddy diffusivity for water vapor
L	Monin-Obukhov length
Q	Source strength
R	Receptor point
R_E	Eulerian velocity autocorrelation coefficient
R_L	Lagrangian velocity autocorrelation coefficient
t	Time
T	Temperature
T_E	Eulerian integral time scale
T_L	Lagrangian integral time scale
u,v,w	Velocity components along the x, y and z axes, respectively
u_*	Friction velocity
v_b	Buoyant velocity
v_g	Gravitational settling velocity
x	Coordinate axis oriented parallel to, and in the same direction as, the mean wind vector
y	Coordinate axis oriented 90° to the left of the mean wind vector
z	Vertical coordinate, positive upward
z_o	Roughness length
$( )'$	Instantaneous deviation from the temporal mean
$(\overline{\ })$	Arithmetic averaging with respect to statistical computations
β	Lagrangian-Eulerian scaling factor
β'	Empirical turbulence scaling factor
Γ	Gamma function
η	Concentration scaling factor
θ	Potential temperature
λ	Wavelength
π	3.14159...
ρ	Density
σ	Standard deviation
σ^2	Variance
τ	Reynold's shearing stress
ϕ	Angle

ACKNOWLEDGEMENTS

The author very gratefully acknowledges the members of his graduate committee for their contributions to this research: Dr. Elmar R. Reiter for his encouragement and helpful suggestions, Dr. Myron L. Corrin for his advice and many hours of stimulating discussions, and Drs. Harry W. Edwards and Donald H. Lenschow for their support and confidence.

The author also wishes to express his most sincere gratitude to Drs. Teizi Henmi and Srinvasan Srivatsangam for their criticisms, suggestions and help in the writing of this manuscript. A very special thank you goes to Mr. John D. Sheaffer for his most valuable assistance in the experimental studies and data analysis.

Many thanks go to Mrs. Grace Holt for her typing and preparation of this manuscript, and to Mrs. Alice Fields for her assistance with the programming. A very warm thank you goes to those numerous other individuals for their many and varied contributions to this project.

This research was supported by the National Science Foundation under Grants GI-44423 and AEN-74-17624-A01.

MODELING ATMOSPHERIC DISPERSION OF LEAD PARTICULATES FROM A HIGHWAY

by

Paul C. Katen

Atmospheric Science Department
Colorado State University
Fort Collins, Colorado

ABSTRACT

In this dissertation we develop a method which will predict the diffusion of lead-bearing particulates emitted by vehicles moving on a highway. The method of modified Gaussian solution, developed through analogy with finite-differencing techniques, when applied to a diffusion equation, fulfills this purpose. This solution meets our demands of accuracy and ease of computation.

It is shown that Gaussian solutions can be applied to the diffusion of gases and particulates emanating from line sources, such as a highway.

We try to establish, through an experimental study, the best method of formulating eddy diffusivity for the short-range dispersion of gaseous pollutants from a line source. This study shows that neither Taylor's statistical theory nor similarity theory yields an appropriate eddy diffusivity. An empirical formula, based on the asymptotic form of Taylor's theory, yields the best results.

A model is then designed, using the method of modified Gaussian solution, for predicting the atmospheric dispersion of particulate lead from a highway. The highway dispersion model employs the results of the gas-diffusion experiments to clarify the role of vehicle-generated turbulence in the dispersion process. The vehicle effects are included as an eddy diffusivity attributable to the moving vehicles and as a buoyancy caused by exhaust heat from the vehicles. The vehicle-generated turbulence and buoyancy are shown to be important in the dispersion process up to about 50 m from the roadway. Thereafter, dispersion is dominated by atmospheric turbulence. A large upward plume spread -- and not the loss of material by deposition -- is primarily responsible for the observed, rapid decrease in concentration with increasing distance from the highway.

1. INTRODUCTION

The contamination of the environment by automobile lead is an important and current national concern. Significant amounts of lead are dissipated into the environment with consequences which are not yet well understood (Lutz, et al., 1970). Three major areas of concern relating to this dissipation are the effects on human health, the environmental consequence of lead contamination, and the interferences of lead with the operation of catalytic emission control devices.

This dissertation has evolved from a project at Colorado State University entitled "Impact on Man of Environmental Contamination Caused by Lead". The overall objective of the project is an assessment of the nature, extent and significance of the environmental contamination by lead. Furthermore, it is expected that the results of this project will be applicable to other atmospheric trace constituents and contaminants (Edwards, 1971, 1972, 1973, and 1974). The project research has centered on two broad areas: the physical and chemical characterization of lead emissions and the description of the processes by which automobile lead moves through the biosphere from its sources to its sinks.

The objectives of our studies on the atmospheric transport of lead have been to investigate:

a) The dispersion of lead generated from highway traffic,

b) The exposure of the urban and suburban populations to airborne lead and,

c) The long-range transport of lead form urban areas.

The purpose of this dissertation is to formulate and apply a model for the short-range atmospheric dispersion of lead-bearing particulates (henceforth referred to as lead particulates) from a highway.

Most of our knowledge concerning dispersion of pollutants from a highway has resulted from studies with gaseous tracers. There have been many model studies for highways and line sources (e.g. Csanady, et al., 1970; Drivas and Shair, 1974), but most of them have not investigated the small scale problems associated with dispersion near the highway.

The dispersion of lead particulates from a highway was investigated by Bezner and Atkins (1970). In investigating the concurrent dispersion of lead and carbon monoxide from a heavily traveled highway, Bezner and Atkins indicated that there was a significant removal of atmospheric lead near the highway. Furthermore, they indicated that most models, then in use, underestimated the vertical transport of pollutants near the highway. However, the models tested did not include any diffusivity attributable to the moving vehicles, nor did they include removal of heavy particulates. To quantify this removal, the deposition of lead near a highway was further studied by Zimdahl (1972). He has established through soil measurements adjacent to Interstate Highway 25 north of Denver, that lead is deposited primarily within 30 meters of the roadway. Beyond this region, soil lead concentrations are indistinguishable from background soil concentrations.

There is considerable variation in particle size emitted from test vehicles even under similar observational conditions (Hirshler, 1957; Habibi, 1970, 1973; Habibi et al., 1970; and Ter Haar et al., 1972). This large particle-size variation, and the observed plume losses indicate that lead must be treated simultaneously as a gas-like particle and as particulate matter. This variation in particle size also indicates that the removal of lead from the dispersing plume is probably occurring simultaneously by gravitational settling and surface deposition. Modelling these characteristics is a formidable task.

The most comprehensive analysis of the short range dispersion of a gaseous pollutant to date was done by Danard (1972). His study considers the dispersion of carbon monoxide from a level roadway. He included the traffic effects on the dispersion with a parameterized eddy diffusivity which was allowed to vary in the direction normal to the highway (x) and upward from the ground (z). The results, which compared a single point measurement with the model predictions, indicate that one needs either to consider the dependence of highway dispersion on additional traffic influences or to consider a more precise parameterization of the vehicular and boundary-layer turbulence.

Some problems specific to the dispersion of pollutants from a highway have recently been studied by Dabberdt (1975, 1976). He reported on a comprehensive measurement program to study the thermal and mechanical effects of vehicular traffic on dispersion from a heavily traveled roadway. These studies have indicated that under the test conditions, the waste heat emissions, the vehicle-induced mixing and a "shelter belt effect" (which is a wind speed reduction created by the "wall" of moving vehicles) are all important dispersion factors.

An earlier analysis by us (Reiter and Katen, 1972), of highway dispersion included the deposition of particulate lead, and resulted in good agreement between the measurements and model predictions. However, that study raised questions as to the validity of using a Gaussian plume model and Taylor's statistical theory to predict vertical dispersion in the atmospheric surface layer. Furthermore, it did not adequately consider the effects of vehicle-generated turbulence on the dispersion from a highway. These shortcomings have been overcome in the present study.

In Chapter 2, we will present and briefly discuss the basics of a few turbulence models as they relate to the dispersion of gases and particulates from a line source, such as a highway, in the atmospheric surface layer.

In Chapter 3, a method of solving two-dimensional, line-source diffusion equations is developed, which is called the method of modified Gaussian solution.† The method is quasi-analytic. It combines u and K_z† profiles with a homogeneous (or Gaussian) solution, instead of combining the variable profiles and the diffusion equation. It is shown that the method of modified Gaussian solution is nearly as accurate as a numerical solution, and is almost as convenient to use as a Gaussian plume model.

In Chapter 4, we try to determine which eddy diffusivity is the most accurate for describing the short range, vertical diffusion from cross-wind line sources in the surface layer. The predictions of the Monin-Obukhov similarity theory, Taylor's statistical theory, and the constant K asymptotic approximation of the statistical theory are compared with measurements.

In Chapter 5, the method of modified Gaussian solution and the results of Chapter 4 are applied to the diffusion of lead emitted on highways, and the predicted concentrations of lead are compared with observations. The method is verified with a series of measurements which were taken at a test site on Interstate Highway 25 about twelve kilometers southeast of Fort Collins, Colorado. Lead concentration and meteorological profiles were measured up to approximately 100 meters downwind from the highway. The survey was conducted during the summer and early fall afternoon hours of 1971 under fair weather conditions typical of the front range of the Rocky Mountains in this season. Samples were not collected under adverse weather conditions. The results of this study should be applicable to most straight, at-grade sections of highways with traffic densities up to about 2500 vehicles per hour.

The conclusions of this study are summarized in Chapter 6, which also contains a set of recommendations for future research.

---

† Please see the preceding list of symbols.

2. Theoretical Background

Three theories are commonly used to describe the turbulent dispersion of pollutants. K theory results from a parameterization of the turbulent flux in terms of an eddy diffusivity, K. Taylor's statistical theory is founded upon Lagrangian statistics of fluid particles in homogeneous turbulent flow fields. Monin-Obukhov similarity theory describes surface layer profiles of meteorological variables in terms of a stability parameter. While the limitations of these theories are severe, they either individually or in concert represent the major thrust of dispersion modeling today. The primary interaction between these three theories arises with the use of the statistical theory or similarity theory to formulate the eddy diffusivities needed in K theory.

This review will be limited to a discussion of the equations pertinent to describe the two-dimensional dispersion of gases and particulates from a cross-wind line source, and will only include the Gaussian (or homogeneous) solutions and a few other analytical solutions for specific surface-layer wind and eddy diffusivity profiles.

Both the Gaussian plume models and the solutions of homogeneous K theory diffusion equations are often applied to similar problems. To avoid confusion we note that, in the following, a Gaussian solution is the homogeneous solution to a governing diffusion equation, and that the Gaussian plume model is an assumed distribution based on the Gaussian or normal distribution (Slade, 1968).

A. K Theory

Many people have reviewed the derivation and assumptions of the K theory differential equations (e.g., Hinze, 1959). Corrsin (1974) advocates that one should avoid the indiscriminate use of K theory. The most serious misapplications of K theory are to the problems of boundary layer shear flows where gradients, and time and length scales usually exceed suggested limiting criteria. (However, in attempting to solve problems outside of an idealized laboratory wind tunnel, or without the use of an extensive computing facility, few, if any, other diffusion theories have proven acceptable.)

The dispersion of a neutrally buoyant gas, or very small particulates with negligible settling velocities, from an infinite cross-wind line source can be described by

$$u(z)\frac{\partial c}{\partial x} = \frac{\partial}{\partial z} K_z(x,z)\frac{\partial c}{\partial z}, \tag{2.1}$$

where c is the concentration of some admixture (gm m^{-3} or parts per million, ppm) and K_z is the eddy diffusivity in the vertical direction ($m^2\ sec^{-1}$). The derivation of Eq. 2.1 from the complete diffusion equation can be found in Sutton (1953). All dependent variables in Eq. 2.1 are considered to be time-averaged. Equation 2.1 includes the K theory parameterization of the turbulent fluxes and also the following assumptions: a) diffusion in the direction of the mean wind is much less than advection by the mean wind ($\frac{\partial}{\partial x} K_x \frac{\partial c}{\partial x} << u\frac{\partial c}{\partial x}$), b) that homogeneity exists in the horizontal cross-wind direction ($\frac{\partial c}{\partial y} = 0$), and c) that steady state conditions ($\partial c/\partial t = 0$) exist.

The simplest solution to Eq. 2.1 arises when the mean wind speed and eddy diffusivity are both steady in time and homogeneous in space. Then Eq. 2.1 simplifies to

$$u\frac{\partial c}{\partial x} = K_z\frac{\partial^2 c}{\partial z^2} \tag{2.2}$$

The solution to Eq. 2.2 (with appropriate boundary conditions) is the homogeneous or Gaussian solution and is given by

$$c = \frac{Q_L}{\sqrt{2\pi}\sqrt{2K_z\, x/u}\ u}\exp\left\{-\frac{1}{4}\frac{z^2}{K_z\, x/u}\right\}, \tag{2.3}$$

where Q_L is the emission rate of the continuous line source (gm m^{-1} sec^{-1}). Part of the reason solutions such as Eq. 2.3 have found so much success in the prediction of the atmospheric dispersion of admixtures is that quite frequently the distribution of diffusing material is observed to follow a normal distribution (Hinze, 1959). Generally, this normal distribution of material might be expected in the free atmosphere, well away from the earth's surface, from the top of the planetary boundary layer, or from the tropopause, or from the stratopause. It is very important to note that while a Gaussian distribution is approximately observed in the atmosphere and it is also the solution to Eq. 2.2, one should not construe this as indicating that the K theory parameterization is correct (Corrsin, 1974). This has lead Corrsin (as quoted by Slade, 1968) to say that the K theory approach is useful in practice but not in theory.

Under oblique wind conditions, the diffusion from the infinite line source must be treated three-dimensionally. The general solution to the three-dimensional diffusion equation can only be obtained by numerical analysis, and requires the parameterization of cross-wind eddy diffusivity. However, Calder (1973) has shown that, in an oblique wind, the solution to the three-dimensional diffusion equation can be approximated well if Eq. 2.3 is modified to account for the angle of the wind to the line source and the increased travel distance to the receptor. Calder's solution is given by

$$C = \frac{Q_i}{\sqrt{2\pi}\ \sigma_z(\frac{x_o}{\cos\phi})\ u\cos\phi}\exp\left(-\frac{z^2}{2\sigma_z^2\ (\frac{x_o}{\cos\phi})}\right), \tag{2.4}$$

where x_o is the perpendicular distance from the line source, σ_z is the standard deviation of the plume distribution, and ϕ is the angle of the wind with respect to the normal to the line source.

A more general solution to Eq. 2.1 for an infinite line source at the surface is given by Sutton (1953) as Eq. 2.5 when u and K_z are given by $u = u_1(z/z_1)^m$ and $K_z = K_1(z/z_1)^n$:

$$c(x,z) = \frac{r\,Q_L}{u_1\,\Gamma(s)}\left[\frac{u_1}{(m-n+2)^2\,K_1\,x}\right]^s \exp\left[-\frac{u_1\,z^{m-n+2}}{(m-n+2)^2\,K_1\,x}\right] \tag{2.5}$$

where $r = m-n+2$, $s = (m+1)/(m-n+2)$, u_1 and K_1 are the wind speed and eddy diffusivity at the reference height, z_1, and Γ is the gamma function (see Abramowitz and Stegun, 1968). This equation was also adapted for conjugate-power law profiles, where $m = 1-n$, which is approximately valid in the constant stress region of the surface layer.

The solution to Eq. 2.1 for an elevated crosswind line source (Walters, 1965; Csanady, 1974) in a constant stress layer is given by

$$c(x,z) = \frac{Q_L}{u_h\, h} \frac{(z/h)^{m/2}}{(2m+1)\frac{K_h x}{u_h\, h^2}} \exp\left\{-\frac{1+\left(\frac{z}{h}\right)^{1+2m}}{(2m+1)^2\frac{K_h\, x}{u_h\, h^2}}\right\} I_{-\frac{m}{2m+1}}\left\{\frac{2\left(\frac{z}{h}\right)^{\frac{2m+1}{2}}}{(2m+1)^2\frac{K_h\, x}{u_h\, h^2}}\right\} \tag{2.6}$$

where h is the line source height, and $I_{-\frac{m}{2m+1}}$ is the Bessel function of imaginary argument and fractional order (see Abramowitz and Stegun, 1968).

The large lead particulates emitted from a vehicle possess a finite gravitational settling velocity, v_g, typically in the range of validity of Stokes Law (Fuchs, 1964). Their dispersion can formally be described by

$$u(z)\frac{\partial c}{\partial x} + v_g \frac{\partial c}{\partial z} = \frac{\partial}{\partial z} K_z(z) \frac{\partial c}{\partial z}. \tag{2.7}$$

Equation 2.7 can also be used to describe the dispersion of a buoyant plume where the plume has a buoyant velocity, denoted by v_b, which replaces v_g in Eq. 2.7. The homogeneous (Gaussian) solution to Eq. 2.7 with appropriate boundary conditions (Pasquill, 1962) is the tilted plume version of Eq. 2.3, and is given by

$$c(x,z) = \frac{Q_L}{\sqrt{2\pi}\,\sqrt{2Kt}\; u} \exp\left\{\frac{(z-v_g t)^2}{4Kt}\right\}, \tag{2.8}$$

where t is the travel time from the source. Several examples of application of this solution are given by Pasquill (1962). The only available analytical solution to Eq. 2.7, with non-constant values for u(z) and $K_z(z)$ was derived by Rounds (1966). The solution is valid for an elevated line source, but only for neutral-stability power law profiles, and will not be considered here.

In some cases, the removal of particulate matter with a small but finite gravitational settling velocity, or of a neutrally buoyant gas, occurs at a rate which is greater than that attributable only to gravitational settling. This removal can be expressed in terms of a deposition velocity. Pasquill (1962) assumes that the rate of deposition is proportional to the concentration near ground level, and that the vertical distribution is unaltered by the process of deposition. The complete concentration profile is then given by replacing the initial source strength by an effective source strength in the homogeneous solution Eq. 2.3. The effective source strength, Q_L', is given by

$$Q_L'(x) = Q_L \exp\left\{-\frac{v_d\; x\; c(x,o)}{Q_L}\right\} \tag{2.9}$$

where Q_L is the initial source strength, v_d is the deposition velocity (m sec^{-1}), x is the downwind distance (meters), and c(x,o) is the concentration at the surface.

B. Formulation of Eddy Diffusivity

To solve diffusion equations, one must specify profiles of wind and eddy diffusivity. The profiles used in the previous section usually do not adequately describe the state of the surface layer.

The prediction of the surface-layer dispersion of pollutants is hindered by flow-field parameters that vary in time and space. The mean wind speed varies very rapidly in the first 10 m of the surface layer. The intensity of turbulence also varies systematically with height above the surface and with the stability of the atmosphere.

Three methods of formulating eddy diffusivity will be developed here and tested in Chapter 4: Monin-Obukhov similarity theory, Taylor's statistical theory, and the asymptotic approximation of Taylor's theory.

i. Monin-Obukhov Similarity Theory

The surface layer, characterized by a region of constant flux of both heat and momentum, has a typical height from 20 to 200 m (Lumley and Panofsky, 1964). Under neutral stability conditions, the mean wind speed u is given by the well-known logarithmic velocity profile

$$u(z) = \frac{u_*}{k} \ell n\left[(z+z_o)/z_o\right], \tag{2.10}$$

where u_* is the friction velocity and is equal to $\left|\frac{\tau}{\rho}\right|^{\frac{1}{2}}$, τ is the Reynolds shearing stress, ρ the density of air, k the von Karman constant, z the vertical coordinate, and z_o the roughness length.

Under non-neutral conditions, surface-layer profiles of meteorological variables can be described as functions of z/L, where L is the Monin-Obukhov Length:

$$L = -\frac{T}{g}\,\frac{u_*^3}{k(\overline{w'T'})}, \tag{2.11}$$

(Monin and Obukhov, 1954) where T is temperature, and g the acceleration due to gravity. In Eq. 2.11 a prime denotes the deviation of an instantaneous value from the time mean, and hence $\overline{w'T'}$ is the temporal correlation between perturbation temperature and vertical velocity. The Monin-Obukhov theory assumes that all non-dimensional surface-layer variables can be expressed as a function of the non-dimensional length z/L. A major accomplishment of micrometeorology in recent years has been to determine empirical formulae relating the fluxes of heat and momentum to temperature and wind profiles. The functional form equations presented below are after Businger (1972), and the numerical coefficients (which in some cases are still questionable) are from Dyer (1974).

$$u = \frac{u_*}{k}\left(\ell n \frac{z}{z_o} - \psi_1\right) \qquad \text{unstable} \tag{2.12a}$$

$$u = \frac{u_*}{k}\left(\ell n \frac{z}{z_o} - \psi_1\right) \qquad \text{stable} \tag{2.12b}$$

$$\theta = \theta_o + \theta_* \left(\ln \frac{z}{z_o} - \psi_2\right) \quad \text{unstable} \quad (2.13a)$$

$$\theta = \theta_o + \theta_* \left(\ln \frac{z}{z_o} - 5\,\frac{z}{L}\right) \quad \text{Stable} \quad (2.13b)$$

$$K_m = k\,u_*\,z\,(1 - 16\,\tfrac{z}{L})^{0.25} \quad \text{unstable} \quad (2.14a)$$

$$K_m = k\,u_*\,z/(1 + 5\,z/L) \quad \text{stable,} \quad (2.14b)$$

where θ is the potential temperature, θ_o is the surface potential temperature, $\theta_* \equiv -\overline{w'T'}/u_*$, K_m is the vertical eddy diffusivity for momentum, $\psi_1 = 2\,\ln[(1+x)/2] + \ln[(1+x^2)/2] - 2\,\tan^{-1}x + \pi/2$, $x = (1-16\,z/L)^{0.25}$, $\psi_2 = \ln[(1+y)/2]$, and $y = (1-16\,z/L)^{0.5}$.

Given a set of temperature and wind profiles, Eqs. 2.12 and 2.13 can be solved iteratively to find u_*, z_o, θ_*, θ_o and L, and, from these, the values of eddy diffusivity. In this study, the eddy diffusivity for momentum, K_m, is assumed to be the diffusivity for the pollutants considered also.

ii. Taylor's Statistical Theory

The underlying principle of Taylor's (1921) approach is that the variance of an ensemble of tracer fluid particles can be given by

$$\sigma_z^2 = 2\,\sigma_{L,w}^2 \int_0^t \int_0^{t'} R_L(\xi)\,d\xi\,dt' \quad (2.15)$$

where $\sigma_{L,w}^2$ is the temporal variance of the Lagrangian vertical wind component, $R_L(\xi)$ is the Lagrangian velocity autocorrelation coefficient and t is the dispersion time. It is assumed that the fluid particles are dispersed from the source such that they have a memory of their past motion up to the time that the Lagrangian autocorrelation coefficient becomes zero. After this time, their motion becomes completely uncorrelated with their previous motion, and they are dispersed completely at random.

Considerable effort has gone into studying the nature of the Lagrangian autocorrelation coefficient, and reviews can be found in the literature (e.g., Lumley and Panofsky, 1964). A scaled Eulerian measurement is generally used instead of the Lagrangian autocorrelation coefficient (Hay and Pasquill, 1959; Corrsin, 1963b; Baldwin and Mickelson, 1962). Hay and Pasquill assume that

$$R_L(\xi) = R_E(t) \quad (2.16)$$

where $\xi = \beta t$, $R_E(t)$ is the measured Eulerian-velocity autocorrelation coefficient, and β is the scaling factor between the correlograms. The Eulerian autocorrelation function is assumed to be of the exponential-decay type given by

$$R_E(t) = \exp(-\,t/T_E), \quad (2.17)$$

where T_E is an appropriate time scale representative of the measured Eulerian autocorrelation coefficient curve. The expression for the plume variance is then given by

$$\sigma_z^2 = 2\,\sigma_w^2\,\beta T_E \left\{t + \beta T_E[\exp(-\,t/\beta T_E) - 1]\right\} \quad (2.18)$$

and the eddy diffusivity, which is related to the variance by $K_z = \frac{1}{2}\frac{d}{dt}(\sigma_z^2)$, is given by

$$K_z = \sigma_w^2\,\beta T_E \left(1 - \exp(-\,t/\beta T_E).\right) \quad (2.19)$$

Taylor's statistical theory is strictly applicable to stationary homogeneous flow fields, for which it was shown by Lumley (1962) that the Lagrangian wind variance is equivalent to the Eulerian measurement of σ_w^2. Much of the experimental work on the study of Taylor's theory has been done in wind tunnels and pipes, which meet the boundary and stationarity conditions. Typically, in these cases, conditions are such that the Lagrangian integral time scale of turbulence, T_L, (Hinze, 1959) is of the order of fractions of a second, and investigations are usually performed anywhere from a few centimeters to a few meters downwind of the sources. Quite unlike the atmosphere, wind tunnels have a turbulence regime that is generally in steady state, with limited eddy scales. Even with the significant differences between wind-tunnel and atmospheric turbulence, Taylor's theory is quite often applied to the atmosphere.

iii. Asymptotic Approximation of Statistical Theory

The third approach to eddy diffusivity estimates that was tested is an empirical formula derived from the asymptotic approximation of Eq. 2.19 (Pasquill, 1962) and is defined by

$$K_z = \sigma_w^2\,\beta' T_E\,. \quad (2.20)$$

where β', an empirically determined free variable, is later shown to be a function of the stability parameter, L. The functional role of the free variable β' in Eq. 2.20 has not been determined. The nature of the experimental measurements, discussed in Chapter 4, does not allow us to assume it to be the same as the Lagrangian-Eulerian time scaling factor β.

For convenience, the eddy diffusivity defined by Eq. 2.20 will be called constant eddy diffusivity, since it does not vary with the diffusion distance (travel time) as Eq. 2.19. In this study "constant" or "variable" eddy diffusivity refers only to the variation of diffusivity with distance downwind of the source and does not imply any restriction on the variation with height above the surface.

The theoretical formulations of eddy diffusivity given above will be used to determine the applicability of K theory with each of the three formulations of eddy diffusivity for describing the short-range vertical diffusion from a cross-wind line source in the surface layer. The emphasis in the analysis, given in Chapter 4, will be to determine whether the diffusion can be described by a constant or variable eddy diffusivity.

3. The Method of Modified Gaussian Solution

The major weakness of the Gaussian solution, described in Chapter 2, is that the wind speed and eddy diffusivity are assumed to be independent of height.

Now we shall develop a method which would allow us to apply Gaussian solutions to problems in which the wind and eddy diffusivity distributions are not homogeneous. Initially, the "stepped Gaussian process" is developed. However, this process is refined because of its shortcomings. The new technique is called the method of modified Gaussian solution. It has the convenience and simplicity of a Gaussian solution, and yet nearly attains the accuracy of a finite difference solution. The method given here is only an approximation. However, this method does offer a quasi-analytic alternative to a numerical solution, with a high degree of accuracy, at a substantial reduction in computer costs.

A. Development of the Method of Modified Gaussian Solution

i. The Stepped Gaussian Process

Let us suppose that a continuous, infinite line source of strength Q_L is located along the y-axis, with the wind blowing in the positive x-direction. If the with wind speed u and eddy diffusivity K_z are constant throughout, the dispersion is described by Eq. 2.2, and its solution is given by Eq. 2.3. For every value of x downwind of the source, Eq. 2.3 predicts a normal or Gaussian distribution of concentration. The question may then be asked: How are two distributions at two different distances downstream related? Since one downstream distribution transforms into the other via the dispersion process, the problem of relating the different downstream distributions to each other can be solved. From statistical theory (Mielke, 1972) it is known that a normal distribution in the x-z plane can be described by the independent variable, $z/(\sqrt{x_i/x_r}\ \sigma(x_r)$, where x_i is the downwind distance to any intermediate point from the real or virtual source, x_r is the distance to any specified receptor and $\sigma(x_r)$ is the standard deviation of the distribution of the pollutant at x_r. In general, points x_i can be considered to lie either upstream or downstream of x_r. The dispersion of a pollutant over a distance x_i can be expressed by the fraction of the standard deviation at x_r as:

$$\sigma(x_i) = \sqrt{x_i/x_r}\ \sigma(x_r). \tag{3.1}$$

Therefore, if a distribution at x_r has a variance $\sigma^2(x_r)$, then a distribution at any point x_i has a variance of $(x_i/x_r)\sigma^2(x_r)$. If the distance x_r is divided into N equal sub-intervals such that $x_r = \sum_{i=1}^{N} (x_i - x_{i-1})$, then the sum of the variances of N successive intermediate points x_i upstream of x_r is equal to the variance of the distribution at x_r. Each fractional interval $(x_i-x_{i-1})/x_r$ contributes its proportional part to the total variance at x_r, since diffusion is additive for variance. This is called the stepped Gaussian process.

Let us apply this stepped Gaussian process on Eq. 2.3. The equation yields a normal distribution in the first intermediate plane at x_r/N. From this distribution a series of virtual sources can be formulated along this plane. The virtual source Q_v at x_r/N and z can be formulated by

$$Q_v(x_r/N,\ z) = c(x_r/N,\ z)\ u\ \Delta z, \tag{3.2}$$

where Δz is the vertical distance between virtual receptor points. The stepped process with N=2 is illustrated in Fig. 3.1. The concentration profile in the plane at $x = 2x_r/N$ is given by the sum of the contributions of each of the virtual sources in the plane x_r/N. This process is repeated a total of N times until the plane at x_r is reached. The agreement between the concentration distributions in a homogeneous field calculated through Eq. 2.3 with $x = x_r$, and by the stepped Gaussian process is excellent.

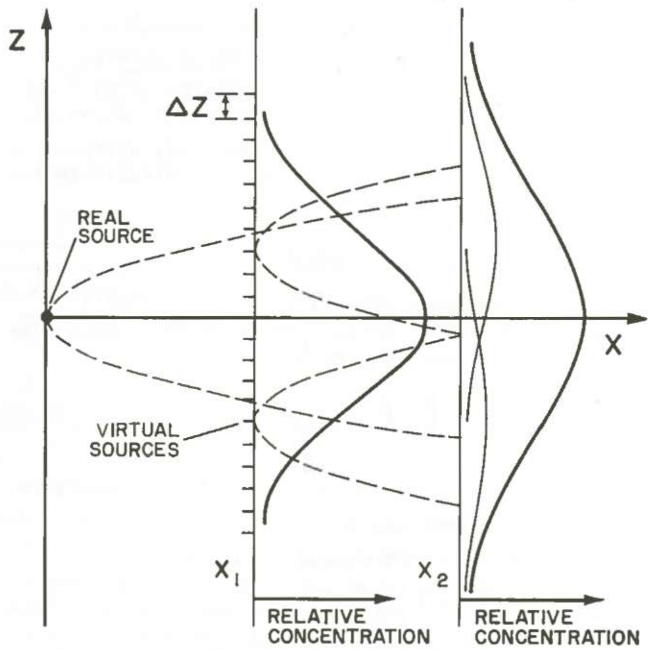

Fig. 3.1. Schematic representation of dispersion by the stepped Gaussian process. The real source at the origin disperses into a normal distribution in the plane at x_1. Virtual sources formulated according to Eq. 3.2 in this plane, two of which are shown, disperse normally in the plane x_2, the sum of all these virtual sources is a normal distribution at x_2.

This stepped Gaussian process can be considered to be analogous to the method of finite differencing. Writing Eq. 2.2, the homogeneous diffusion equation, in finite difference form (Van Buijtenen et al., 1973) gives

$$c(i,j) = c(i,j-1) + \frac{K\Delta x}{u\Delta z^2}\Big(c(i+1,j-1) + c(i-1,j-1) - 2c(i,j-1)\Big), \tag{3.3}$$

where i, j represent grid locations along the z and x directions, respectively. The finite difference computations are limited by a numerical stability criterion. That is, Δx and Δz must satisfy the expression given by

$$6 \frac{K\Delta x}{u} \leq \Delta z^2, \quad (3.4)$$

(Richtmyer and Morton, 1967). Equation 3.3 is used operationally by proceeding with computations along the direction from grid point to grid point. The stepped Gaussian process also leads to a set of forward marching calculations. It can be shown that computations by the numerical methods lead to a nearly normal distribution of pollutant concentration. In the case of the stepped Gaussian process, the computations lead to exactly normal distributions by assumption (see Fig. 3.1).

ii. Stepped Gaussian Process Applied to an Inhomogeneous Wind Field

The stepped Gaussian process can also be applied to a flow field where wind speed and eddy diffusivity are functions of height. To use the stepped Gaussian process in this case we must include the vertical variation of u and K_z in the evaluation scheme. When u and K_z are functions of height, Eq. 2.1 can be expressed in finite difference form as

$$c(i,j) = c(i,j-1) + \frac{\Delta x}{u_i \Delta z} \left(K_{i+\frac{1}{2}} \frac{c(i+1,j-1)-c(i,j-1)}{\Delta z} - K_{i-\frac{1}{2}} \frac{c(i,j-1)-c(i-1,j-1)}{\Delta z}\right), \quad (3.5)$$

(Cotton, 1976), which demonstrates that gradients in u and K_z must be considered in the evaluation. When the Gaussian solution is used in a stepped process, one can allow the downstream step size, x_i, to approach zero. In that limit it would be possible to use the Gaussian solution as if the inhomogeneous field were a series of sub-fields of homogeneous flow. The dispersion from each virtual source is evaluated with the values of u and K_z representative at the point of each virtual source. However, for practical applications x_i cannot be made infinitesimally small. Thus, as in Eq. 3.5, the vertical variations in u and in K_z must be used in the Gaussian solution in the stepped process. An analysis has shown that for each source and receptor pair (real or virtual), the geometric means of u and of K_z† between a source level and a receptor level must be used in the Gaussian solution to give the concentration at that specific receptor. These geometric means represent the "effective" values of these variables over the region between the source and receptor. One should note that, in the limiting case of $x_i \rightarrow 0$, the geometric means between source and receptor levels will approach the values of u and of K_z at the source level.

It was found that the stepped Gaussian process was, within limits, insensitive to the magnitude of x_i. If x_i is not larger than about 2 m and the vertical grid spacing is about 0.1 m, the concentration profiles obtained by the stepped Gaussian process agree with those obtained by numerical differencing.

However, if the step size x_i is greater than 2 m, the effective values of u and K_z can no longer be approximated by the geometric means of u and K_z at the source and receptor. As a result, the concentration profiles predicted by the method become different from those predicted by numerical differencing.

Therefore, it is necessary to improve the stepped Gaussian process by improving the method of estimation of the effective values of u and K_z.

iii. The Method of Modified Gaussian Solution

When one writes the diffusion equation in a finite difference form and divides the continuous space into a series of discrete grid points, one can show that the pollutant is dispersed into a specific region of the grid space. This region is determined by the second order difference equation (3.5) and it is marked by large dots in Fig. 3.2. Furthermore, only specific portions of this region play a role in determining the concentration at any single receptor point. The three regions outlined by the boxes in Fig. 3.2, are the "fields of influence"" for each of the indicated receptor points. This figure demonstrates that only the values of u and K_z at certain grid points, those within each box, will be involved in the calculations of the concentration at each of the specified receptors. When Eq. 3.5 is solved iteratively, one can see that there is a hierarchy in the importance of the terms in the solution. From a comparison of the magnitudes of the terms in the solution, one can neglect some of the terms and one can determine an "effective field of influence" for each of the receptor points. This effective field of influence is considered to be the region of the flow field which most strongly influenced the dispersion for that receptor point. These effective fields of influence are then used to calculate the effective values of u and K_z. These effective values are geometric means over the effective field of influence, and they are then used to determine the concentration at specific receptor points by direct evaluation of the Gaussian solution Eq. 2.3.

There are probably many methods of determining the effective field of influence, and in Appendix A the empirical technique which was developed is presented. The effective field of influence, in general, encompasses the region between the source and receptor levels and extends on either side of the encompassed region.

B. Application of the Method of Modified Gaussian Solution

In this section it will be shown that the method of modified Gaussian solution is as versatile as the Gaussian plume model, and that its accuracy is comparable to the numerical or analytical solution to several of the commonly occurring dispersion problems.

i. Plume Reflected at the Surface

The above discussion is based on the assumption that no substantial interaction occurs between the diffusing material and any plume-reflecting boundary. For situations where a diffusing plume is intercepted by an impenetrable boundary, such as the earth's surface or an inversion lid, the "method of images" is often used (Sutton, 1953; Turner, 1964; Slade,

† The geometric means of u and K_z are given by $(u_s u_r)^{\frac{1}{2}}$ and $(K_s K_r)^{\frac{1}{2}}$, respectively, where s and r denote the values at the source and receptor levels.

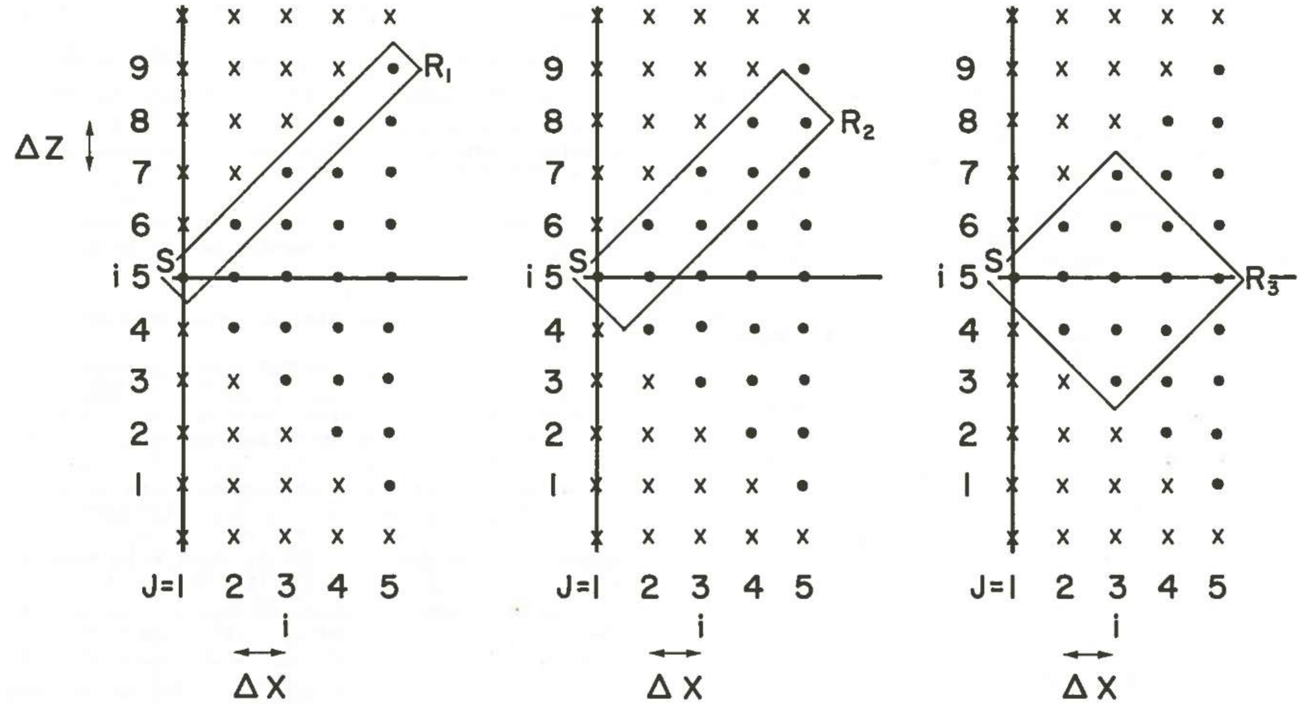

Figure 3.2. Schematic representation of a two-dimensional finite differencing grid in the x-z plane. Wind is assumed to blow from left to right with the source, S, at i-5, j=1. The portion of the grid to which material can disperse according to Eq. 3.5 is marked by dots (·). The specific "fields of influence" for the three indicated receptor points, R_i, i = 1,2,3 are outlined.

1968). The equation used for describing the dispersion from a cross-wind line source, near the surface is given by

$$c = \frac{Q_L}{\sqrt{2\pi}\,\sigma_z u} \exp\left(\left(-\left(\frac{(z-h)^2}{2\sigma_z^2}\right) + \exp -\left(\frac{(z+h)^2}{2\sigma_z^2}\right)\right)\right) \quad (3.6)$$

where h is the height of the source above the surface.

Numerical experiments showed that it is not necessary to mirror the wind and eddy diffusivity profiles in the surface, and that it is only necessary to determine the effective values of the field variables for the "real" source at each specific receptor point according to the technique suggested in Appendix A. The effective values calculated for the real source can then be substituted into the image term.

Let us consider the following example: The source is at a height of 5m; and the profiles of wind speed and eddy diffusivity are respectively given by $u = 0.7 \ln(z) + 4.04$ and $K_z = \sigma_w^2 T_E$ where $\sigma_w = 0.082 \ln(z) + 0.33$ and $T_E = 0.62 \ln(z) + 2.25$. The source strength, Q_L, is 5.2 cc m^{-1} sec^{1}. Figure 3.3 shows a comparison of the predictions of the concentrations by the finite-difference method, the modified Gaussian solution and the Gaussian plume model. The numerical solution uses a no-flux boundary condition at the surface, whereas the method of modified Gaussian solution and the Gaussian plume model use the method of images. These distributions were calculated at a distance of 300 m downwind of the source. The Gaussian plume model was evaluated with the values of u and K_z at the source height. The concentration distribution predicted by the method of the modified Gaussian solution is in excellent agreement with the numerical solution of Eq. 2.1. Additional data are given in Table 3.1. The table shows good agreement with respect to conservation of mass (within 1.5%), location of the center of gravity and plume variance.

ii. Sources Near the Surface

A second commonly encountered problem is a cross-wind line source at or near the surface of the earth. The solution for the case of a cross-wind line source at the surface with wind and eddy diffusivity approximated by power law profiles is given by Eq. 2.4 (Sutton, 1953). In order to solve numerically the diffusion equation for this situation, it is necessary to assume that the source is not exactly at the surface, but at the lowest grid level. Thus, zero wind speeds and eddy diffusivities at the surface are not encountered. This is generally an acceptable approximation and has little effect on the final solution. An analytical solution to the case of a cross-wind line source near the surface, with the wind and eddy diffusivity approximated by power law profiles, is given by Eq. 2.5. The corresponding numerical solution using the finite differencing scheme given by Eq. 3.5 can be used for virtually any type of profiles for u and K_z, but generally is difficult to use operationally.

Figure 3.4 presents a comparison of the predictions made by the finite difference method, the method of modified Gaussian solution and the Gaussian solution (Eq. 2.5). For purposes of illustration, the Gaussian solution is evaluated with u and K_z representative of three different levels: 0.2 m, 2.2 m,

$$6 \frac{K\Delta x}{u} \leq \Delta z^2, \tag{3.4}$$

(Richtmyer and Morton, 1967). Equation 3.3 is used operationally by proceeding with computations along the direction from grid point to grid point. The stepped Gaussian process also leads to a set of forward marching calculations. It can be shown that computations by the numerical methods lead to a nearly normal distribution of pollutant concentration. In the case of the stepped Gaussian process, the computations lead to exactly normal distributions by assumption (see Fig. 3.1).

ii. Stepped Gaussian Process Applied to an Inhomogeneous Wind Field

The stepped Gaussian process can also be applied to a flow field where wind speed and eddy diffusivity are functions of height. To use the stepped Gaussian process in this case we must include the vertical variation of u and K_z in the evaluation scheme. When u and K_z are functions of height, Eq. 2.1 can be expressed in finite difference form as

$$c(i,j) = c(i,j-1) + \frac{\Delta x}{u_i \Delta z} \left(K_{i+\frac{1}{2}} \frac{c(i+1,j-1)-c(i,j-1)}{\Delta z} - K_{i-\frac{1}{2}} \frac{c(i,j-1)-c(i-1,j-1)}{\Delta z} \right), \tag{3.5}$$

(Cotton, 1976), which demonstrates that gradients in u and K_z must be considered in the evaluation. When the Gaussian solution is used in a stepped process, one can allow the downstream step size, x_i, to approach zero. In that limit it would be possible to use the Gaussian solution as if the inhomogeneous field were a series of sub-fields of homogeneous flow. The dispersion from each virtual source is evaluated with the values of u and K_z representative at the point of each virtual source. However, for practical applications x_i cannot be made infinitesimally small. Thus, as in Eq. 3.5, the vertical variations in u and in K_z must be used in the Gaussian solution in the stepped process. An analysis has shown that for each source and receptor pair (real or virtual), the geometric means of u and of K_z† between a source level and a receptor level must be used in the Gaussian solution to give the concentration at that specific receptor. These geometric means represent the "effective" values of these variables over the region between the source and receptor. One should note that, in the limiting case of $x_i \to 0$, the geometric means between source and receptor levels will approach the values of u and of K_z at the source level.

It was found that the stepped Gaussian process was, within limits, insensitive to the magnitude of x_i. If x_i is not larger than about 2 m and the vertical grid spacing is about 0.1 m, the concentration profiles obtained by the stepped Gaussian process agree with those obtained by numerical differencing. However, if the step size x_i is greater than 2 m, the effective values of u and K_z can no longer be approximated by the geometric means of u and K_z at the source and receptor. As a result, the concentration profiles predicted by the method become different from those predicted by numerical differencing.

Therefore, it is necessary to improve the stepped Gaussian process by improving the method of estimation of the effective values of u and K_z.

iii. The Method of Modified Gaussian Solution

When one writes the diffusion equation in a finite difference form and divides the continuous space into a series of discrete grid points, one can show that the pollutant is dispersed into a specific region of the grid space. This region is determined by the second order difference equation (3.5) and it is marked by large dots in Fig. 3.2. Furthermore, only specific portions of this region play a role in determining the concentration at any single receptor point. The three regions outlined by the boxes in Fig. 3.2, are the "fields of influence"" for each of the indicated receptor points. This figure demonstrates that only the values of u and K_z at certain grid points, those within each box, will be involved in the calculations of the concentration at each of the specified receptors. When Eq. 3.5 is solved iteratively, one can see that there is a hierarchy in the importance of the terms in the solution. From a comparison of the magnitudes of the terms in the solution, one can neglect some of the terms and one can determine an "effective field of influence" for each of the receptor points. This effective field of influence is considered to be the region of the flow field which most strongly influenced the dispersion for that receptor point. These effective fields of influence are then used to calculate the effective values of u and K_z. These effective values are geometric means over the effective field of influence, and they are then used to determine the concentration at specific receptor points by direct evaluation of the Gaussian solution Eq. 2.3.

There are probably many methods of determining the effective field of influence, and in Appendix A the empirical technique which was developed is presented. The effective field of influence, in general, encompasses the region between the source and receptor levels and extends on either side of the encompassed region.

B. Application of the Method of Modified Gaussian Solution

In this section it will be shown that the method of modified Gaussian solution is as versatile as the Gaussian plume model, and that its accuracy is comparable to the numerical or analytical solution to several of the commonly occurring dispersion problems.

i. Plume Reflected at the Surface

The above discussion is based on the assumption that no substantial interaction occurs between the diffusing material and any plume-reflecting boundary. For situations where a diffusing plume is intercepted by an impenetrable boundary, such as the earth's surface or an inversion lid, the "method of images" is often used (Sutton, 1953; Turner, 1964; Slade,

† The geometric means of u and K_z are given by $(u_s u_r)^{\frac{1}{2}}$ and $(K_s K_r)^{\frac{1}{2}}$, respectively, where s and r denote the values at the source and receptor levels.

levels of the distribution. It is felt that these errors could be substantially reduced if the scheme suggested in Appendix A for determining the effective values was slightly modified for cases when the receptor point is in the upper portion (the tail) of the distribution. Further work is needed to improve the method in this respect.

TABLE 3.2

Comparison of conservation of mass, Q, location of the center of gravity with respect to the source height, C.G., and plume variance, σ^2, for the modified Gaussian and numerical solutions to Eq. 2.5. Source height, z_h, is 0.2m, x = 300 m, and $u = 2.69(z/z_h)^{0.16}$ and $K_z = 0.02(z/z_h)^{0.84}$.

	Q(gm $m^{-1}sec^{-1}$)	C.G. (m)	$\sigma^2(m^2)$
Numerical	5.2	4.6	39.60
Modified Gaussian	5.7	4.91	43.0

iii. Particulates with a Gravitational Settling Velocity

The dispersion of particulate matter, which possess a non-negligible settling velocity, is described by Eq. 2.7. This particular formulation of the problem does not include the effect of the gravitational settling velocity on eddy diffusivity (Pasquill, 1962). It does, however, describe clearly the phenomenon of gravitational settling.

Under homogeneous conditions, the solution to Eq. 2.6 is the tilted plume equation (Eq. 2.7). The validity of this solution is often doubted when non-homogeneous conditions are encountered. However, this analysis shows that by using Eq. 2.7 in the method of modified Gaussian solution, one can obtain an excellent approximation to the numerical solution of Eq. 2.6.

A comparison of the concentration distribution predicted by finite difference method, by the method of modified Gaussian solution and by the Gaussian solution is given in Fig. 3.5. The Gaussian solution uses u and K_z representative at the source height. In this example the source height, z_h, was 10.2 m and the initial source strength was 5.2 gm m^{-1} sec^{-1}. The particulates were assumed to have a settling velocity, v_g, of 0.2 m sec^{-1}. The profiles of wind speed and eddy diffusivity are respectively $u = 5.0(z/z_h)^{0.16}$ and $K_z = 0.6(z/z_h)^{0.84}$. Good agreement between the concentration distributions predicted by the methods of finite difference and modified Gaussian solution is seen in Fig. 3.5 and Table 3.3. In comparing these statistics one must consider that there has been a substantial loss of mass from the profile due to gravitational settling. The predictions of the methods of finite difference and of modified Gaussian solution agree with respect to the location of the center of gravity (C.G.) and variance of the distributions.

Since the method used for determining the effective field of influence depends on plume size and location, several techniques were tested to account for the vertical displacement of the plume centerline due to particulate settling. In the examples tested, no significant improvement in the predicted profile was obtained by attempting to account for this vertical displacement of the plume centerline.

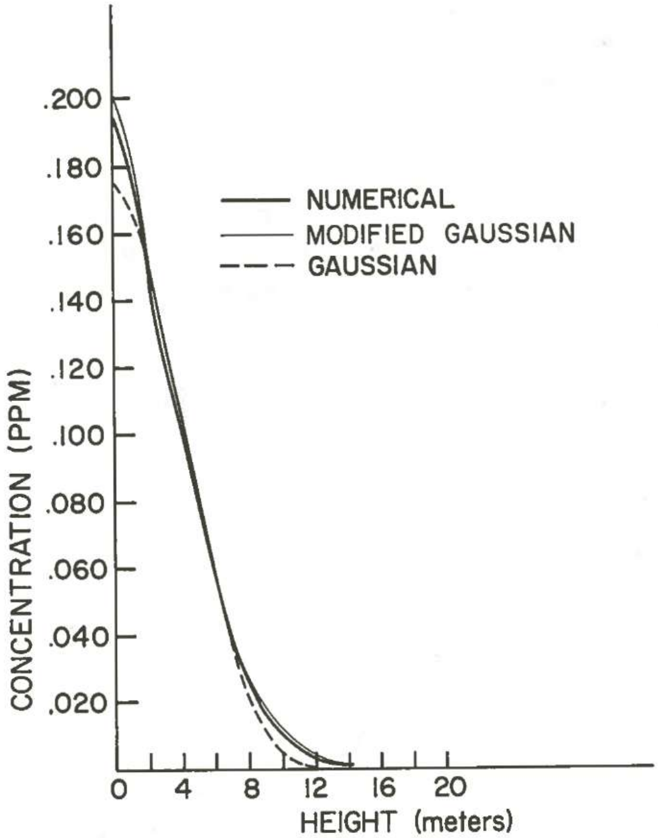

Figure 3.5. A comparison of the numerical solution, the modified Gaussian solution and the Gaussian solution to Eq. 2.6. The Gaussian solution is evaluated with u and K_z representative of the source height, z_h, 10.2 m. The initial source strength was 5.2 gm m^{-1} sec^{-1}, x = 300 m, v_g = -0.2 m sec^{-1}, $u = 5.0(z/z_h)^{0.16}$ and $K_z = 0.6(z/z_h)^{0.84}$.

TABLE 3.3

Comparison of the conservation of mass, Q, location of the center of gravity and the variance of the numerical and modified Gaussian solutions to Eq. 2.6 for a source at 10.2 m, v_g = -0.2 m sec^{-1}, x = 300 m, $u = 5.0(z/z_h)^{0.16}$ and $K_z = 0.6(z/z_h)^{0.84}$.

	Q(gm $m^{-1}sec^{-1}$)	C.G. (m)	$\sigma^2(m^2)$
Numerical	3.13	-3.72	42.11
Modified Gaussian	3.23	-3.81	42.14

However, under other conditions, the results might be different from those obtained here through Appendix A.

C. Summary

The numerical examples presented here have shown the applicability of the method of modified Gaussian solution to predict concentration profiles in inhomogeneous flow fields. Since only certain regions of the flow field dominate in the determination of the concentration at a point, it is possible to determine the effective values of the flow field variables for that receptor point. Once the effective values of u and K_z have been determined for a specific receptor point, one is able to compute the concentration at that point using the Gaussian solution. The accuracy of this method is comparable to that of the finite difference method. With this method of modified Gaussian solution, the major characteristics of a dispersing plume in a shear flow are accurately predicted, as they are in studies which use more sophisticated modeling techniques. These include the shape of the distribution curve, the point of maximum concentration, the center of gravity, the variance and the total mass.

Several special cases, including the effects of surface plume reflection, gravitational settling and a near-surface source, also yielded accurate predictions with the method of modified Gaussian solution. Each of these cases has a homogeneous solution which can be used with the effective values of the field variables, u and K_z, to yield the solution to the inhomogeneous case. While there is room for improvement in the determination of the effective values for the flow field variables, the method is very useful, and satisfactorily fills the gap between the homogeneous Gaussian solution and the more accurate finite difference method.

The uniqueness of the technique developed here lies in part in that the Gaussian solution is a solution to the diffusion equation and also in that the operational nature of the method of modified Gaussian solution is analogous to those of a finite difference marching solution. The solution technique, while approximate, does offer a high degree of accuracy at a substantial reduction in computer costs.

4. LINE SOURCE GAS-DIFFUSION EXPERIMENTS

This chapter investigates the accuracy of several different methods of predicting the dispersion of a gaseous pollutant from a crosswind line source in the atmospheric surface layer. This study is important for the development of a model of the dispersion of lead particulates from a highway. It is also important, in its own right, for a better understanding of the vertical diffusion of a contaminant in the surface layer.

Each of the basic K theory differential equations given in Chapter 2 requires the inclusion of a profile of eddy diffusivity (K_z) in order to describe the dispersion. The dispersion of a pollutant from a highway depends on atmospheric as well as vehicle-induced turbulence. To separate these effects, one must first investigate atmospheric eddy diffusivity.

The question to be answered here is: Which formulation of eddy diffusivity -- the Monin-Obukhov similarity theory, Taylor's statistical theory or the constant K, asymptotic approximation of Taylor's statistical theory -- is the most accurate in predicting the short-range, vertical spread of pollutants in the surface layer? This study will compare predictions made by these three theories to a set of measurements. Once a method of parameterizing atmospheric eddy diffusivity is formulated, one can use it as a basis from which to infer the vehicular effects.

A. Design of the Gas-Diffusion Experiment

The gas diffusion experiment was designed so that the results could readily be compared to the two-dimensional model predictions.

In the tests, sulfur hexaflouride (SF_6) was released from an elevated, effectively "infinite" line source. (The "infinite" length is to satisfy the conditions of cross-wind homogeneity.) In all tests, the line source had a strength of 4.8 cc m^{-1} sec^{-1} of sulfur hexafluoride (at ambient conditions). Vertical concentration profiles were measured at three relatively short distances downwind. The details of the experimental equipment and data processing are described in Appendix B. Figure 4.1 shows the experimental setup.

For these tests, the line source was positioned at either 6.5 or 2.8 meters above the surface, and was attached to a steel cable which was stretched taut between three supporting towers. The former position (6.5 m) was designed to keep the diffusing plume away from the surface, as much as possible, over the sampling range. Thus, one is able to observe the rate of spread of the plume before the plume interacts with the surface. Under these conditions, the eddy diffusivity which best describes the growth of plume can be accurately determined. The second position (2.8 m above the surface) was to observe the behavior of the plume in the critical region near the surface. Comparison of the data and model predictions are used to determine how well K theory, the method of modified Gaussian solution and the method of images (which is used when the plume intersects the surface) perform under these conditions.

Three sampling towers were positioned approximately in a line perpendicular to the line source and parallel to the anticipated mean wind direction. The meteorological measurements consisted of the horizontal wind, vertical wind fluctuations and temperature. The middle sampling tower was also used to mount bivane anemometers. Detailed plane and cross-sectional views are given in Figs. 4.2 and 4.3, respectively. The test site, located at the Colorado State University airport, was approximately 250 meters downwind of several buildings, whose effect on the measured profiles is discussed below. The terrain was slightly inclined (a 1.5 m elevation increase over 250 m) and the surface covering, which varied slightly with the season, was mainly rye grass approximately 50 cm tall.

B. Discussion of the Gas Diffusion Data

Figures 4.4a through 4.4j present the measured atmospheric profiles for each of the ten case studies. These figures include profiles of the mean wind speed, standard deviation of the vertical wind component, and

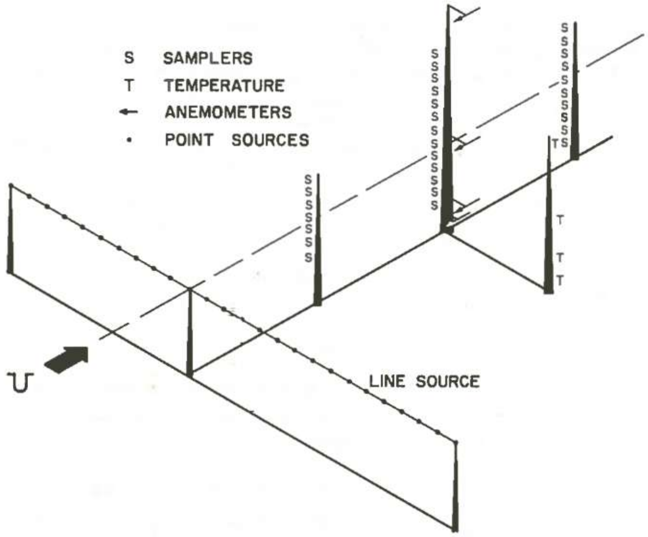

Figure 4.1. Design of the line source gas-diffusion experiment at the CSU airport. Figure shows the approximate placement of the line source, the sampling locations (S), anemometers and thermocouples (T).

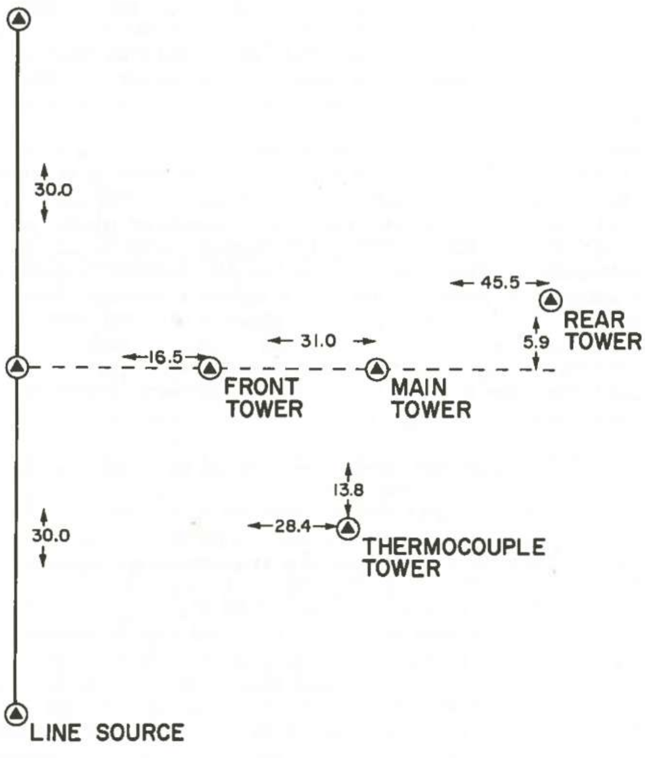

Figure 4.2. Plan view of the test site equipment for the gas-diffusion experiment.

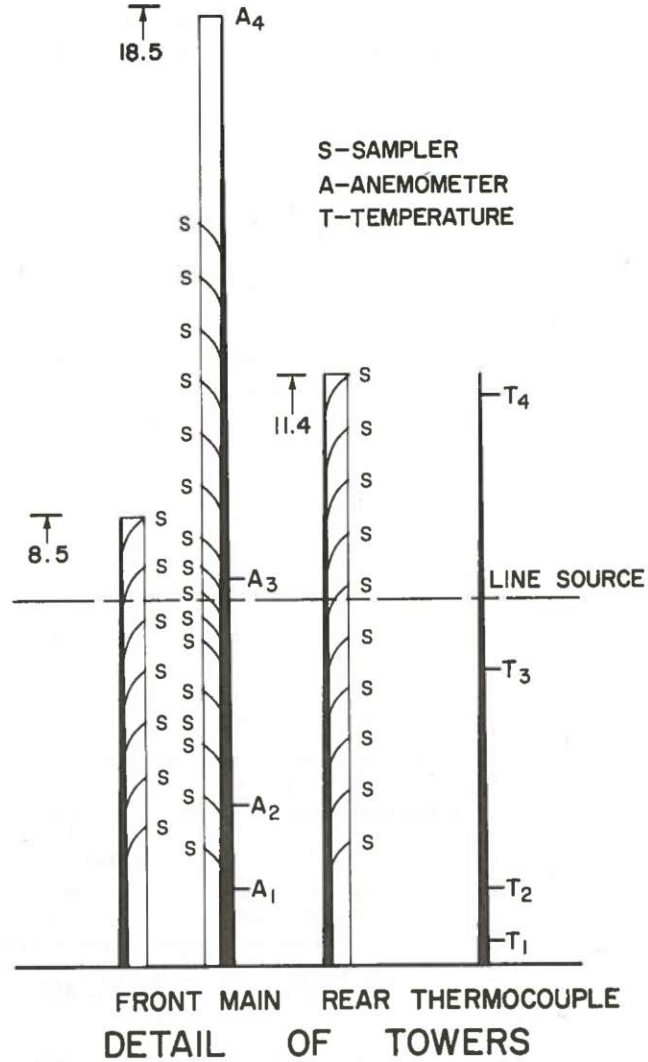

Figure 4.3. Cross-section view of the site equipment for the gas-diffusion experiment.

an Eulerian integral time scale derived from the Eulerian vertical-velocity autocorrelation coefficient. Included on some of these graphs are the uncorrected bivane and UVW anemometer vertical-wind standard deviations. The purpose of including these data is to demonstrate the validity of the algorithm derived to correct the errors associated with the bivane vertical wind component measurement. These corrections are discussed further in Appendix B. In general, the agreement between the corrected bivane and UVW anemometers, is excellent. Table 4.1 gives additional data on the experimental conditions. These include the mean wind direction with respect to the normal to the line source (ϕ), the friction velocity (u_*), the roughness length (z_0) and the Monin-Obukhov length (L) for each of the ten test cases.

In about 20% of the curves in Fig. 4.4, there are some discrepancies between the measured values and the fitted logarithmic or power law curves (of the form $A \propto z^{\alpha}$) for u, σ_w, or T_E at the upper level anemometer (18.5 m). These discrepancies are not due to instrumental error. They result from a change in roughness

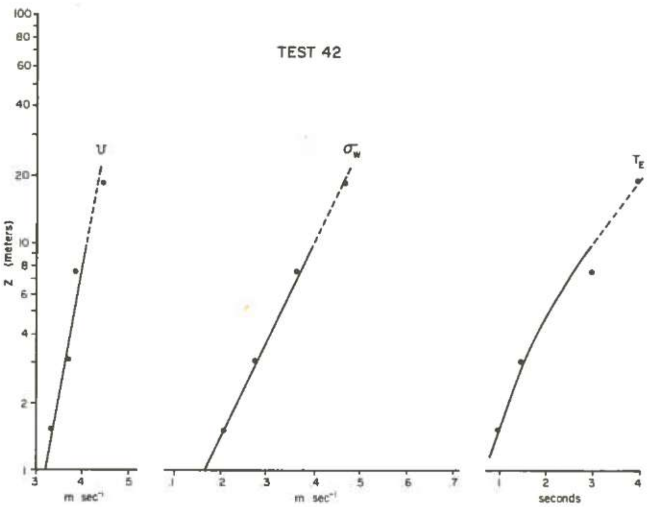

Figure 4.4a. Measured boundary layer profiles of wind speed, u, vertical wind standard deviation, σ_W, and Eulerian integral time scale, T_E, for Test 42.

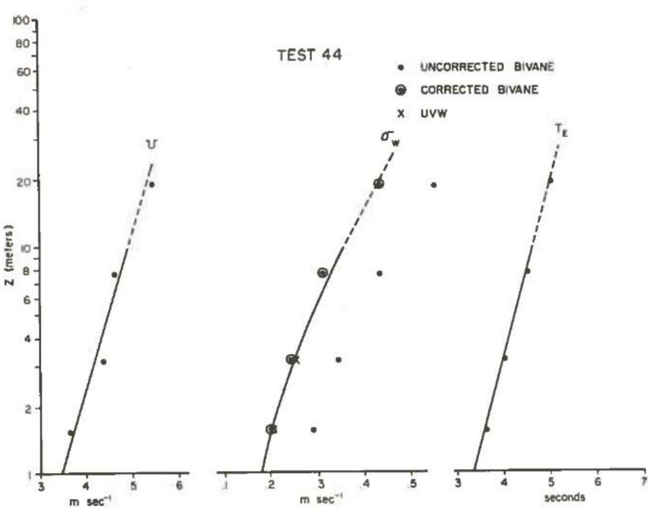

Figure 4.4b. Measured boundary layer profiles of wind speed, u, vertical wind standard deviation, σ_W, and Eulerian integral time scale, T_E, for Test 44. Included on the profiles for the vertical wind standard deviation are the uncorrected bivane anemometer values, (•), the corrected bivane values, (ʘ), and the UVW anemeometer values, (x).

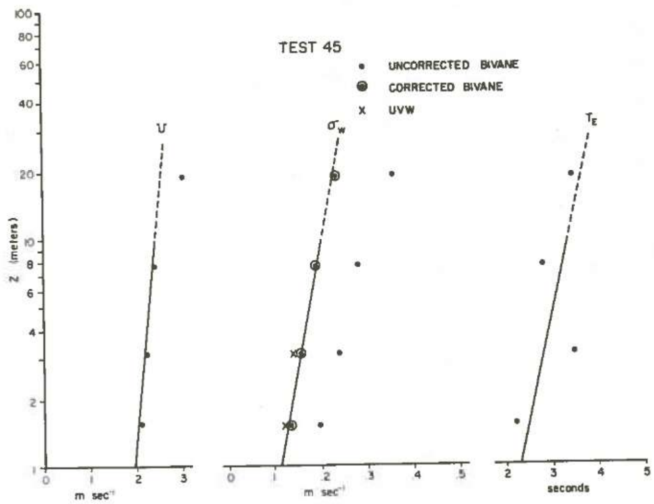

Figure 4.4c. Same as Fig. 4.4b except for Test 45.

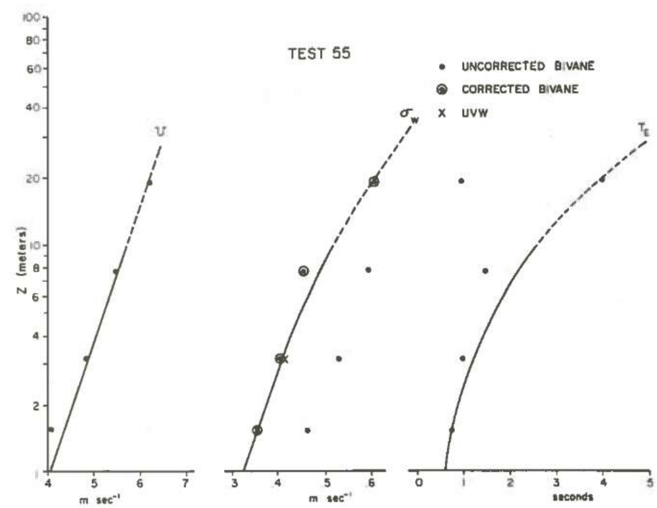

Figure 4.4d. Same as Fig. 4.4b except for Test 55.

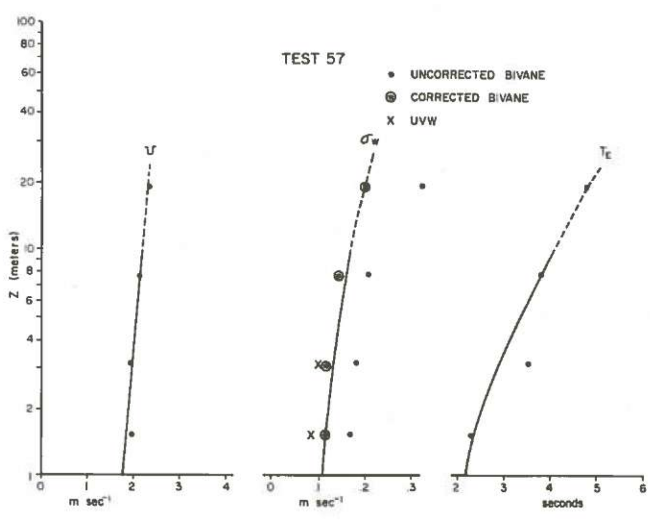

Figure 4.4e. Same as Fig. 4.4b except for Test 57.

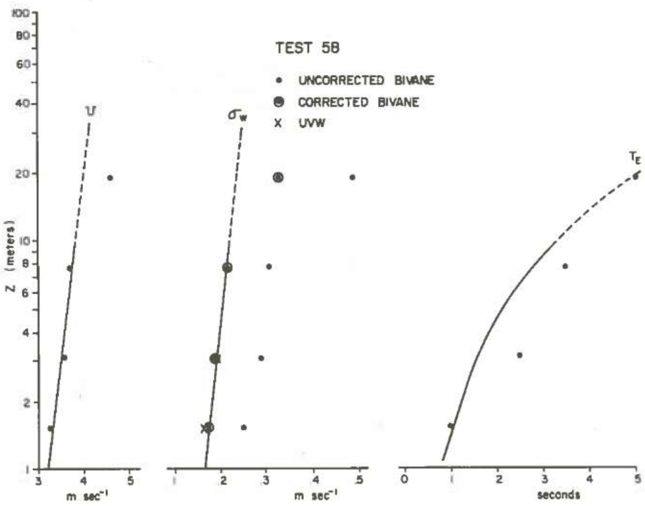

Figure 4.4f. Same as Fig. 4.4b except for Test 58.

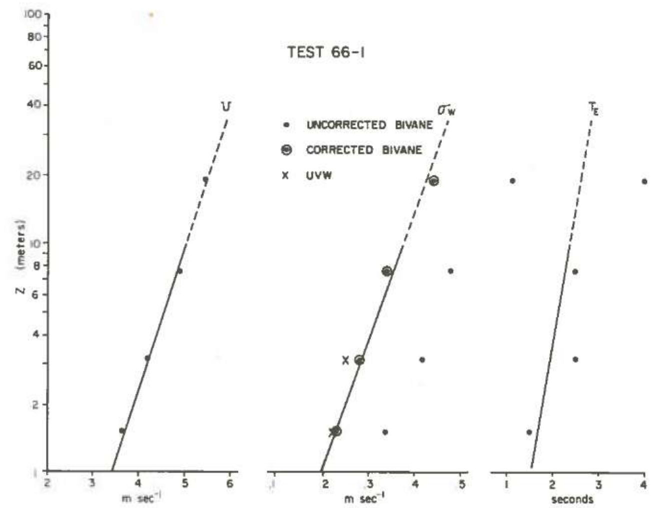

Figure 4.4i. Same as Fig 4.4b. except for Test 66-1.

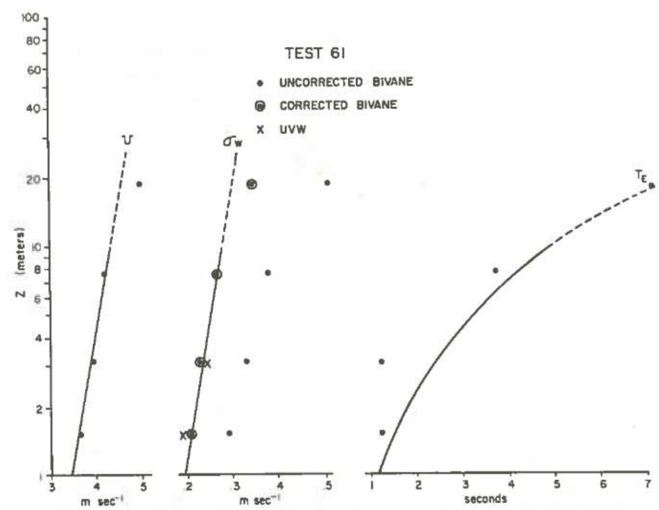

Figure 4.4g. Same as Fig. 4.4b except for Test 61.

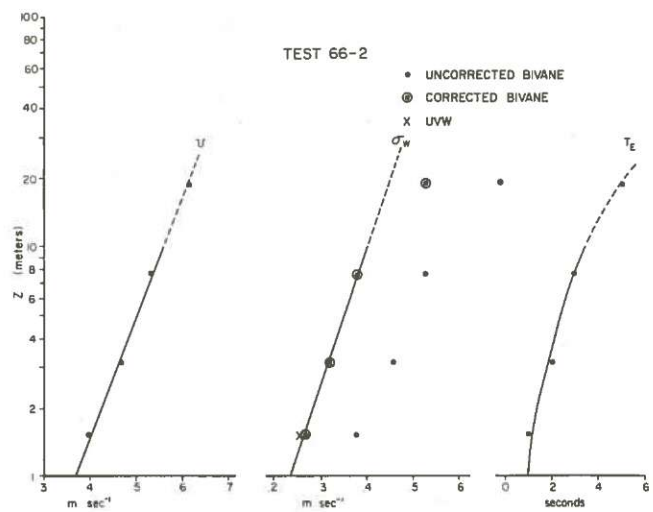

Figure 4.4j. Same as Fig. 4.4b except for Test 66-2.

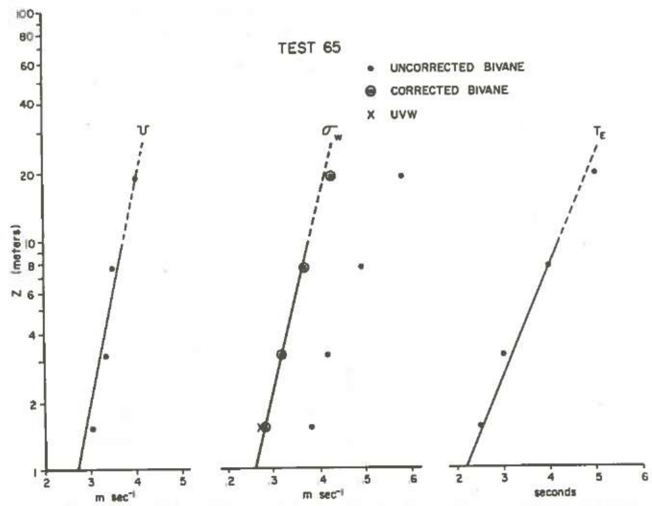

Figure 4.4h. Same as Fig. 4.4b except for Test 65

TABLE 4.1

The mean wind direction with respect to the normal to the line source, the friction velocity, the roughness length, and the Monin-Obukhov length for each of the ten gaseous diffusion experiments.

DATE	TEST	ϕ(deg)	u_*(m sec^{-1})	z_o(cm)	L(m)
5/23/74	42	18.3	0.26	0.3	- 3.3
6/03/74	44	15.4	0.27	0.6	-22.6
6/05/74	45	10.8	0.16	0.4	- 8.0
9/06/74	55	5.0	0.25	0.4	27.2
10/29/74	57	4.5	0.14	0.5	- 9.6
11/01/74	58	5.0	0.26	1.0	-14.9
11/07/74	61	6.0	0.32	1.3	- 7.5
6/02/75	65	18.0	0.23	0.9	-14.3
6/05/75	66-1	6.0	0.39	3.0	-23.9
6/05/75	66-2	7.4	0.42	3.0	-35.8

elements (buildings and trees) upwind of the airport test site. This indicates that the vertical profiles are in the process of adjusting to the smooth airport surface, but that these changes have not, in all cases, reached the 18.5 m measurement level. These slight differences between the measurements and fitted profiles will not significantly affect the predicted concentration profiles.

In the first seven test cases discussed here (Tests 42, 44, 45, 55, 57, 58, and 61, see Appendix B), given in Figs. 4.5 through 4.11, the line source was positioned 6.5 m above the surface. Vertical inhomogeneities in the wind speed and eddy diffusivity profiles only slightly skew the distributions (see Figs. 4.5 through 4.11).

In the last three test cases (Tests 65, 66-1, and 66-2), given in Figs. 4.12, 4.13, and 4.14, respectively, the source was positioned 2.8 m above the surface. Six of the tests (Tests 42, 44, 45, 65, 66-1, and 66-2), have two concentration profiles measured at 16.5 m and 31 m downwind. These are denoted by a and b, respectively, in the figures. The remaining four tests (Tests 55, 57, 58, and 61) have, in addition to the first two profiles, a third profile at 45.5 m, which is denoted by c in the figures.

The measured concentration profiles, in Figs. 4.5 to 4.14, appear to be generally correct. However, some of the measured curves show slight irregularities in their shape as, for example, in Figs. 4.6b, 4.7b, 4.10a, and 4.11b (in Tests 44, 45, 58, and 61, respectively). The likely sources of experimental error are discussed in Appendix B.

Some slight differences between the actual line-source strength (4.8 cc m^{-1} sec^{-1}) and the source strength computed from the measured concentrations, as given in Table 4.2, are attributable to wind profile smoothing or truncation of the upper edge of the profiles.

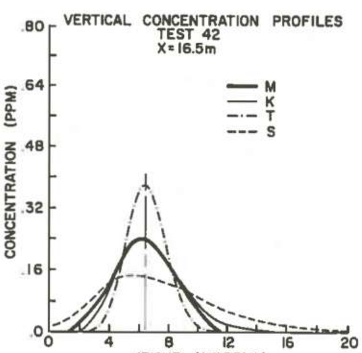

Figure 4.5a. Comparison of the measured (M) and predicted profiles for Test 42 using Similarity theory (S), Taylor's theory (T) and the constant K asymptotic approximation of Taylor's theory (K) to formulate the eddy diffusivity. Source height was 6.5 m and the distance downstream of the source was x = 16.5 m.

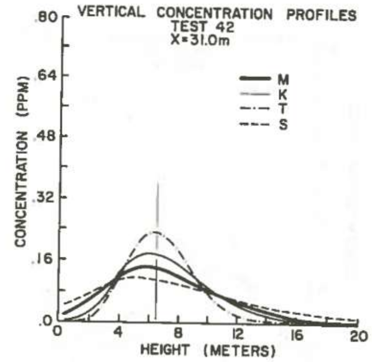

Figure 4.5b. Same as Fig. 4.5a except with x = 31.0 m.

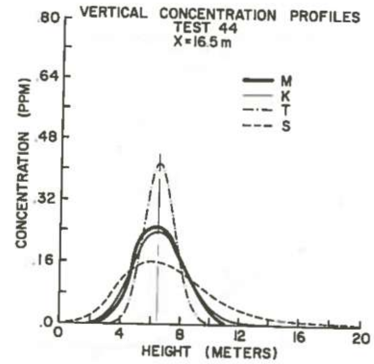

Figure 4.6a. Same as Fig. 4.5a except for Test 44 with x = 16.5 m.

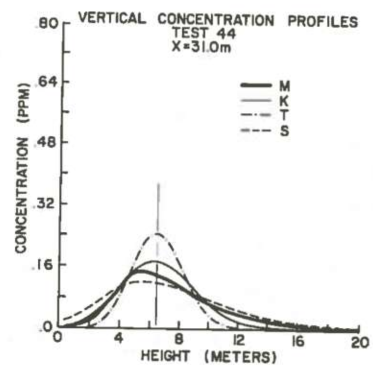

Figure 4.6b. Same as Fig. 4.5a except for Test 44 with x = 31.0 m.

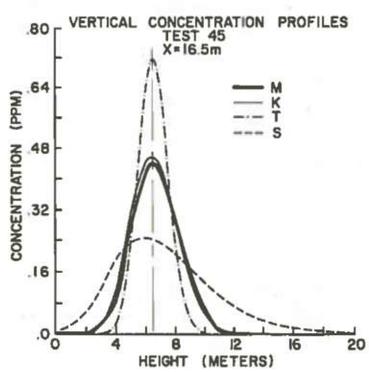

Figure 4.7a. Same as Fig. 4.5a except for Test 45 with x = 16.5 m.

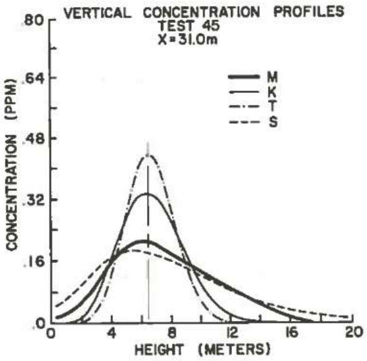

Figure 4.7b. Same as Fig. 4.5a except for Test 45 with x = 31.0 m.

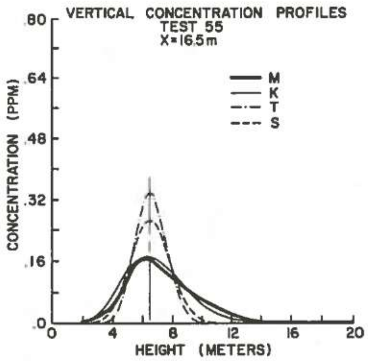

Figure 4.8a. Same as Fig. 4.5a except for Test 55 with x = 16.5 m.

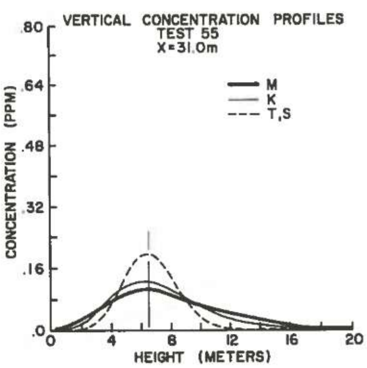

Figure 4.8b. Same as Fig. 4.5a except for Test 55 with x = 31.0 m.

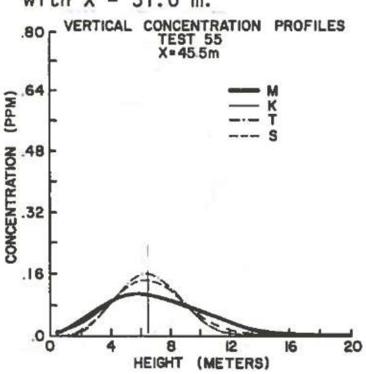

Figure 4.8c. Same as Fig. 4.5a except for Test 55 with x = 45.5 m.

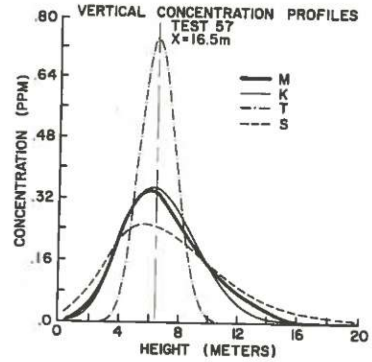

Figure 4.9a. Same as Fig. 4.5a except for Test 57 with x = 16.5 m.

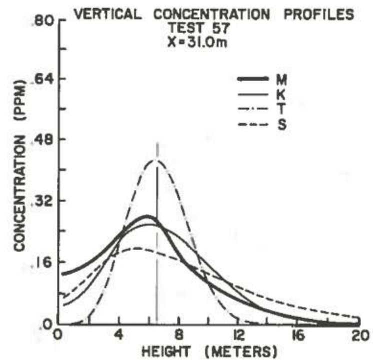

Figure 4.9b. Same as Fig. 4.5a except for Test 57 with x = 31.0 m.

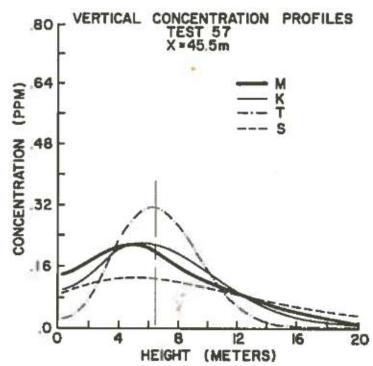

Figure 4.9c. Same as Fig. 4.5a except for Test 57 with x = 45.5 m.

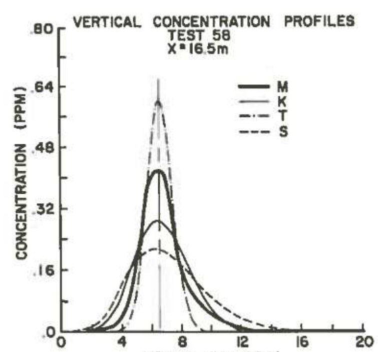

Figure 4.10a. Same as Fig. 4.5a except for Test 58 with x = 16.5 m.

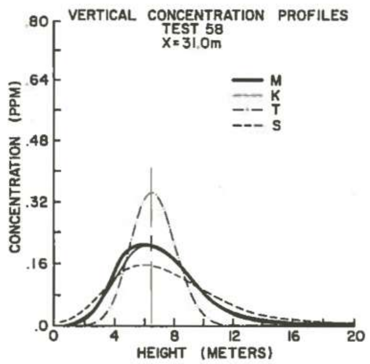

Figure 4.10b. Same as Fig. 4.5a except for Test 58 with x = 31.0 m.

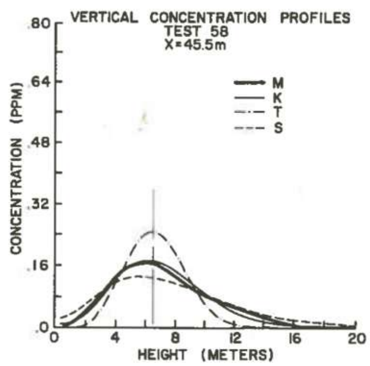

Figure 4.10c. Same as Fig. 4.5a except for Test 58 with x = 45.5 m.

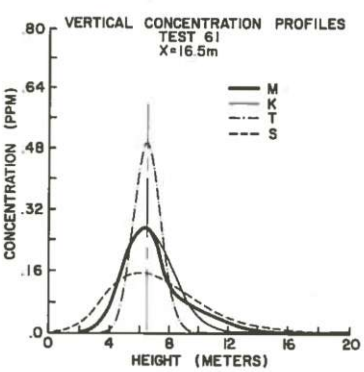

Figure 4.11a. Same as Fig. 4.5a except for Test 61 with x = 16.5 m.

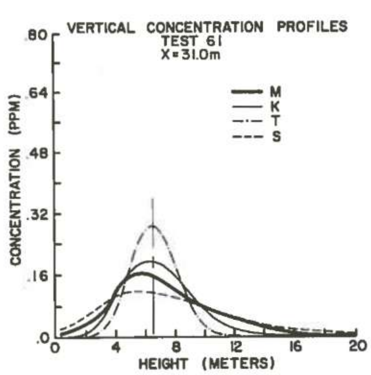

Figure 4.11b. Same as Fig. 4.5a except for Test 61 with x = 31.0 m

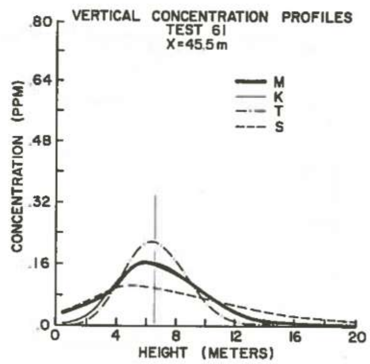

Figure 4.11c. Same as Fig. 4.5a except for Test 61 with x = 45.5 m.

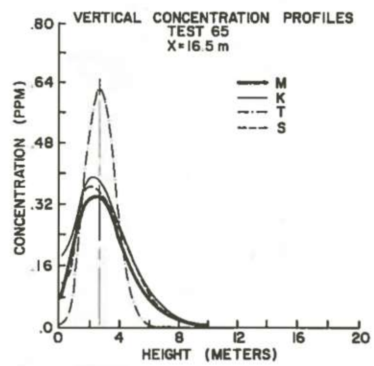

Figure 4.12a. Same as Fig. 4.5a except for Test 65 with a source height of 2.8 m and x = 16.5 m.

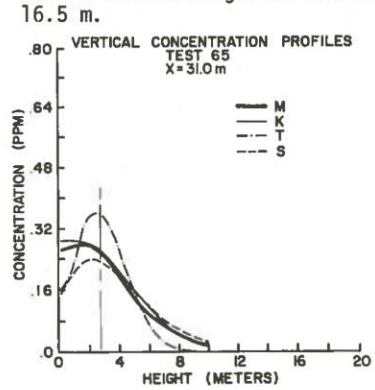

Figure 4.12b. Same as Fig. 4.5a except for Test 65 with a source height of 2.8 m and x = 31.0 m.

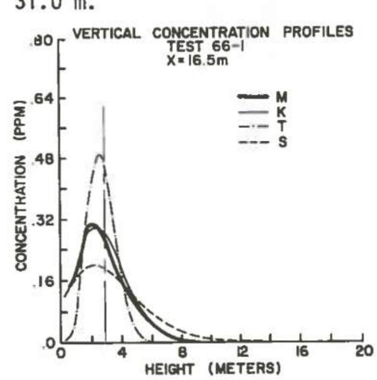

Figure 4.13a. Same as Fig. 4.5a except for Test 66-1 with source height of 2.8 m and x = 16.5 m.

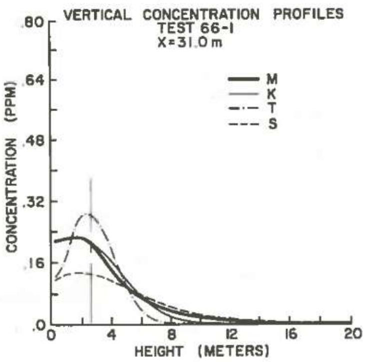

Figure 4.13b. Same as Fig. 4.5a except for Test 66-1 with a source height of 2.8 m and x = 31.0 m.

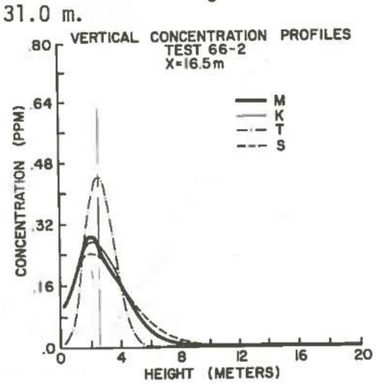

Figure 4.14a Same as Fig. 4.5a except for Test 66-2 with a source height of 2.8 m and x = 16.5 m.

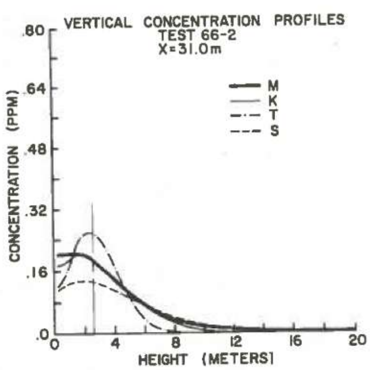

Figure 4.14b. Same as Fig. 4.5a except for Test 66-2 with a source height of 2.8 m and x = 31.0 m.

TABLE 4.2

Comparison of measured profiles (M) and the modified Gaussian solutions to Eq. 2.1 using: a) the constant K eddy diffusivity given by Eq. 2.20 (K), b) similarity theory (S), and c) Taylor's theory (T). The table includes figures on the total mass associated with each distribution, location of maximum concentration and center of gravity with respect to source level, and the variance of the distribution.

TEST	β'	x(m)	curve	Q	Z_{MAX}(m)	Z_{CG}(m)	$\sigma_Z^2(m^2)$
42	1.11	16.5	M	4.71	-0.2	0.03	3.79
			K	4.73	-0.2	0.48	4.69
			S	4.86	-0.8	1.05	14.18
			T	4.77	0.0	0.17	1.79
		31.0	M	4.77	-0.7	0.68	11.79
			K	4.71	-0.5	0.77	8.83
			S	4.71	-2.0	1.39	20.53
			T	4.70	0.0	0.37	4.68
44	1.0	16.5	M	4.76	-0.1	0.14	2.41
			K	4.76	-0.1	0.22	3.22
			S	5.06	-0.4	0.72	8.72
			T	4.79	0.0	0.12	1.05
		31.0	M	4.78	-1.2	0.77	9.77
			K	4.74	-0.3	0.32	6.00
			S	5.08	-1.0	1.02	15.18
			T	4.78	-0.1	0.18	3.00
45	1.27	16.5	M	4.75	0.0	0.27	2.52
			K	4.76	-0.1	0.19	2.51
			S	5.00	-0.6	0.86	10.74
			T	4.79	0.0	0.12	1.03
		31.0	M	4.79	-0.4	1.12	11.50
			K	4.72	-0.1	0.29	4.57
			S	4.90	-0.7	1.18	17.45
			T	4.77	0.0	0.17	2.76
55	2.5	16.5	M	4.63	-0.3	0.78	4.92
			K	4.78	-0.3	0.44	4.45
			S	4.72	-0.1	0.10	1.74
			T	4.81	0.0	0.12	1.12
		31.0	M	4.80	-0.3	1.20	11.70
			K	4.77	-0.5	0.69	8.50
			S	4.70	-0.1	0.11	3.19
			T	4.78	-0.1	0.22	3.26
		45.5	M	4.79	-0.6	0.41	8.97
			K	4.82	-0.7	0.81	12.35
			S	4.67	-0.2	0.13	4.57
			T	4.74	-0.3	0.37	5.95
57	4.1	16.5	M	4.79	-0.3	0.62	8.05
			K	4.72	-0.3	0.42	6.36
			S	4.84	-0.9	1.00	13.88
			T	4.81	0.0	0.13	1.43
		31.0	M	4.77	-0.7	-0.15	12.58
			K	4.74	-0.5	0.59	11.64
			S	4.68	-2.1	1.35	20.30
			T	4.76	-0.1	0.23	4.22
		45.5	M	4.80	-1.7	0.65	19.67
			K	4.78	-1.0	0.71	15.83
			S	3.88	-1.5	1.94	25.60
			T	4.73	-0.3	0.36	7.84
58	3.35	16.5	M	4.80	0.0	0.26	2.18
			K	4.76	-0.1	0.30	3.30
			S	4.76	-0.4	0.64	6.50
			T	4.80	0.0	0.11	0.74
		31.0	M	4.85	-0.5	0.39	6.48
			K	4.73	-0.3	0.47	6.14
			S	4.79	-0.5	0.94	12.16
			T	4.77	0.0	0.14	2.22
		45.5	M	4.79	-0.7	0.71	10.25
			K	4.73	-0.4	0.60	9.05
			S	4.77	-1.1	1.14	16.30
			T	4.74	-0.1	0.22	4.11
61	1.4	16.5	M	4.74	-0.1	0.49	4.22
			K	4.76	-0.1	0.28	2.89
			S	4.76	-0.5	0.83	9.61
			T	4.79	0.0	0.11	0.86
		31.0	M	4.80	-0.5	0.71	9.66
			K	4.73	-0.2	0.44	5.39
			S	4.77	-1.1	1.13	16.27
			T	4.77	0.0	0.17	2.47
		45.5	M	4.80	-0.9	0.16	8.49
			K	4.73	-0.2	0.56	7.92
			S	4.63	-2.1	1.36	20.08
			T	4.73	-0.1	0.26	4.36

Table 4.2 Continued.

Test	β'	x(m)	curve	Q	Z_{MAX}(m)	Z_{CG}(m)	$\sigma_Z^2(m^2)$
65	2.48	16.5	M	4.41	-.03	0.42	3.08
			K	4.76	-0.7	0.34	3.16
			S	4.85	-0.5	0.52	3.22
			T	4.73	-0.1	0.11	0.98
		31.0	M	4.55	-1.1	0.51	4.84
			K	4.63	sfc	0.56	4.88
			S	4.22	-0.5	0.99	5.41
			T	4.50	-0.3	0.26	2.63
66-1	2.25	16.5	M	4.52	-0.6	0.34	2.74
			K	4.72	-0.4	0.32	2.43
			S	4.33	-0.5	0.99	5.46
			T	4.75	0.0	0.15	0.87
		31.0	M	4.82	-0.8	1.04	8.01
			K	4.57	-1.0	0.56	4.30
			S	3.98	-0.8	2.03	11.61
			T	4.47	-0.2	0.28	2.26
66-2	2.5	16.5	M	4.53	-0.5	0.30	2.54
			K	4.81	-0.5	0.40	2.81
			S	4.78	-0.7	0.67	4.02
			T	4.75	-0.1	0.14	0.90
		31.0	M	4.79	-0.9	1.05	7.12
			K	4.73	-1.4	0.75	5.42
			S	4.07	-0.7	1.77	10.01
			T	4.50	-0.3	0.29	2.34

The Gaussian plume model is, of course, mass conservative, whereas, as seen in Table 4.2, the method of modified Gaussian solution shows a small deviation from a full conservation of mass. This is due to the approximation used to determine the effective values of the field variables. Three other important statistics for the measured and predicted distributions are also presented in Table 4.2: The center of gravity of each distribution (C.G.); the location of its maximum concentration (z_{max}); and the variance of each distribution (σ^2). When looking at this table, one should remember that the characteristics of dispersion in a boundary layer shear flow are such that: a) the center of gravity of the distribution moves upward with time, and b) the point of the maximum concentration moves downward toward the surface.

C. Analysis of the Gas-Diffusion Data

The 24 sets of data given in Figs. 4.5 to 4.14 show: a) that two-dimensional K theory (Eq. 2.1) is sufficiently accurate for describing surface-layer gas diffusion; and b) that there is agreement between the measured concentrations and the predictions made using Eq. 2.20, the constant K, asymptotic approximation of Taylor's theory.

In reviewing all the 24 sets of data in Figs. 4.5 to 4.14, one sees that the constant K formulation (lines "K" in the diagrams), $K_z = \sigma_w^2 \beta' T_E$, gives the best agreement in 18 of the 24 data sets. The factor β' was assumed to be a constant in the vertical and down-stream directions for each individual experiment. β' may be a function of z, but the data are currently insufficient to prove this. The dependency of β' on stability will be described in the next section.

Two of the six remaining profiles, which did not agree with the predictions made with the constant K formulation, agree with the similarity theory prediction (S). Three of the six, Figs. 4.5b, 4.6b, and 4.11b, lie between the predictions of the similarity theory and the constant K theory. The sixth curve, Fig. 4.10a, is a very narrow plume, and the measured values lie between the predictions of the constant K and Taylor's (T) theories. Test case 55, given in Fig. 4.8, is the only stable case studied. In this case, both similarity and Taylor's theories severely underestimate the dispersion.

A more detailed analysis of the data reveals that the profiles predicted by the method of modified Gaussian solution with Eq. 2.20 are indeed skewed, and that in most cases, the predictions quite closely parallel the measurements. The data in Table 4.2 show that both the measured and predicted distributions have a nearly full conservation of mass. Furthermore, they show that there are some slight disagreements between the locations of the measured and predicted peak concentrations. However, one sees a trend in the data by which the location of the maximum concentration is displaced downward below the release height as predicted by theory.

The center of gravity and variance statistics are not as sensitive to small errors in plume positioning as the other statistics and are thus better indicators of the shape of the distribution. These statistics, also presented in Table 4.2, further verify the similarity of the measured and predicted distributions.

D. Dependence of Scale Factor β' on Stability

The scale factor β' in Eq. 2.20 is a proportionality constant which is determined for each test case to give the best comparison between the sets of measured and predicted profiles. Figure 4.15 relates β' to the absolute value of the Monin-Obukhov length, L, which is a measure of the convective stability of the boundary layer. There is some scatter in the data as seen in the figure. With the exception of one point, the lower group of data points are from the three earliest tests (conducted prior to the summer of 1974). It is felt that the data from the more recent tests, forming the upper group, are the more accurate, due to improvements in the field measurements and laboratory techniques. This stability dependent curve will be used in the analysis of the highway data.

E. The Effect of β on Predicted Plume Width

These data which show that Taylor's statistical theory underestimates diffusion must be considered to be an important conclusion. To further substantiate this conclusion one can use a simple approximation to cross-check the result.

Both the factors β and β' in Eqs. 2.19 and 2.20, respectively, are proportionality constants whose values are determined empirically. β is, by Eq. 2.16, a scaling factor between the Eulerian and Langrangian integral time scales, whereas the eddy diffusivity in Eq. 2.20 varies linearly with β'. In this scaling role, β does not have as significant an effect on the predicted plume width as β', and thus the value of β is not critical to the conclusion mentioned in the above paragraph. This can be illustrated as follows. Pasquill (1962) demonstrated that for short diffusion times, Eq. 2.18 can be approximated by

$$\sigma_z^2 = \sigma_w^2 t^2 , \tag{4.1}$$

where t = x/u. This equation gives the maximum plume width predicted by Taylor's statistical theory at any point (diffusion time) a short distance downwind of the source.

One can evaluate Eq. 4.1 using the values σ_w and u at the source height to estimate the maximum plume

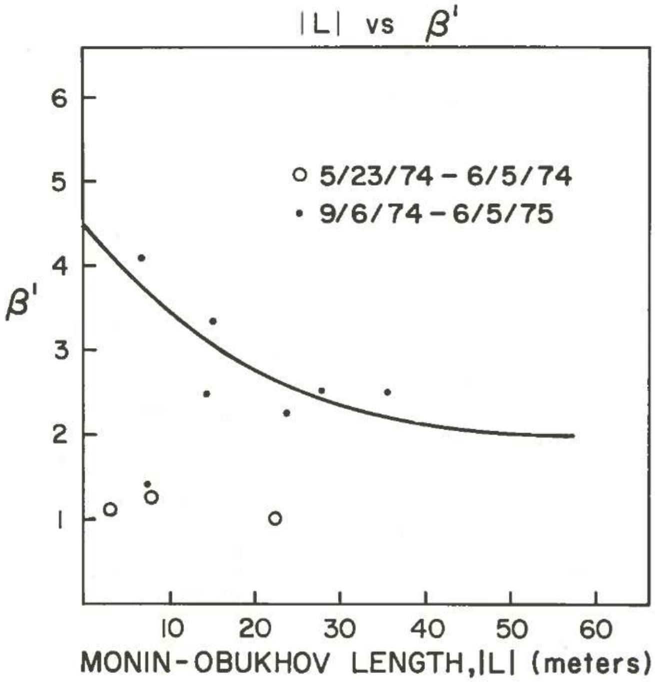

Figure 4.15. Relationship between β' and the absolute value of the Monin-Obukhov length.

width. The comparison of these predicted variances with the measured values in Table 4.2 shows that, in all cases, Taylor's statistical theory underestimates the diffusion.

F. Summary

In this chapter we analyzed the data from an extensive field program designed to study vertical diffusion in the surface layer. These test data were compared to the predictions by three formulations of eddy diffusivity. The results showed that the similarity and statistical theories do not accurately predict the diffusion of gas in the surface layer. The most accurate predictions of diffusion were given by an empirical parameterization based on the constant K asymptotic approximation of statistical theory and this formulation will be used to describe the eddy diffusivity of the unperturbed surface layer in the modelling of the dispersion of lead particulates from a highway.

5. Modeling the Dispersion of Lead Particulates From a Highway

In the previous chapters, investigations were conducted into each of the components important for solving the equation which describes the short-range, surface-layer dispersion of lead particulates from a highway. From comparisons of the Gaussian and numerical solutions of a diffusion equation, a new methodology was developed. It was shown that gaseous tracers from line sources diffusing in the surface layer are not described well with either statistical theory or similarity theory. An accurate prediction of tracer concentration can, however, be given by the constant K asymptotic approximation of statistical theory (Eq. 2.20).

Here the results of the previous chapters are used as bases on which to construct a model of the short-range transport of particulate lead released by automobiles.

A. Field Program

The site selected for conducting the field studies was on a section of the north-south Interstate Route 25. The site was located 12 km southeast of Fort Collins, Colorado in an area where background lead aerosol concentrations were low. The section of roadway selected was straight and had a grade of 1.5% with the uphill traffic (south-bound) in the lane nearest to the equipment. The segment of the road along which the test equipment was located was nearly "level" for about 200 m. One problem with this sampling site was that there was a frontage road 10 m to the west of the highway. However, this little-used road presented no problem during any of the sampling periods for no vehicles traveled along this road during any of the tests.

The aim of the measurement program was to obtain down-wind lead concentration and meteorological parameter profiles in a plane perpendicular to the highway. The placement of the measuring equipment is described in Appendix B. Sampling was limited to the first 100 m from the highway, for here gravitational settling and surface deposition results in the removal of some of the lead-particulates. This was seen in previous atmospheric measurements (Besner and Atkins, 1970) and soil measurements (Zimdahl, 1971). Beyond the 100 m limit it is difficult to collect a significant amount of lead on a high volume filter in a 30 minute sampling period. Samples were averaged for 30 minutes so that lead concentrations could be related to nearly steady atmospheric conditions.

B. Source Parameterization

i. Vehicle Lead Emissions

In dispersion modeling, one of the most crucial factors is an accurate determination of the source strength and its spatial and temporal distribution. Lead emission from a single vehicle has a large range, dependent upon operating conditions (Hirchler, 1957) and the age of the vehicle (Habibi, 1970). There is also a considerable variation among vehicles operating under the same conditions (Habibi, 1973). In formulating a model for lead diffusion, the average of the available data on lead emissions (e.g. Habibi, 1970, 1973; Habibi, et al., 1970; Hirshler, 1957; and Ter Haar, et al., 1972) was used. No studies have been conducted for determining the effect of altitude on lead emissions, and near-sea-level values had to be used, although the field tests were conducted at about 1,500 m above sea level.

The operating condition of the vehicles along the test section of the highway was assumed to be steady state at speeds between 55 and 70 mph. These tests were conducted prior to the reduction of maximum speed limit to 55 mph. Under low speed, stop-and-go, city-type driving conditions, considerable lead residue can be accumulated in the exhaust system with only 20% to 60% of the consumed lead being emitted. Previous investigations (Hirshler, 1957; Ter Haar, et al., 1972; and Habibi, 1970) generally agree that while the lead emissions vary significantly with operating conditions, the difference between the average emission and typical city-type driving emission is usually exhausted under high-speed driving or during high speed, full-throttle accelerations. The net result is that, overall, between 70 and 80% of the consumed lead is exhausted from the vehicle. High speed operation is very close to this equilibrium state with about 70% emission rate (Habibi, et al., 1970). The remoteness of the test site from urban areas meant that the vehicle emission rates could be considered to be stabilized due to operating conditions. The majority of the vehicles passing the sampling station would have been operating continuously at high-speed conditions for a considerable distance.

ii. Particle-Size Classification

The physical characteristics of vehicular lead emissions have been extensively studied. For an "aged" lead aerosol, measured some distance from its source, Robinson and Ludwig (1967) found a mass median equivalent diameter (mmed) of 0.25 μm. Ter Haar reported 35% of the emissions were less than 0.5 μm and 40% by weight were more than 5.0 μm in diameter (aerodynamic equivalent diameter for a unit density sphere). Typically, the sub-micron fraction may represent from 5 to 50% of the quantity emitted, but generally lies between 20 and 25% of the consumed lead.

Particle size distributions were further studied by Corrin and Menne (1975) in a series of Anderson impactor studies at varying distances from a roadway. Their results showed that between 60 and 80% of the collected particles were less than one micron in diameter and 10 to 20% of the collected particles were greater than 8 μm, but these results gave no clear picture of the average size distribution either at a given distance from the roadway, or any systematic variation of particle size with distance from the roadway.

In a set of wind tunnel experiments, Habibi (1973) found that the deposits collected from the floor represented about 10% of the consumed lead. Since these particles ranged in diameter from 5 μm to 3000 μm, a combination of gravitational settling and surface impaction were probably responsible for their removal. The fraction of particulate lead found in the range from sub-micron to about 10 μm has also been observed to vary from a few percent to 40% of the consumed lead, but normally about 35%.

Because of the wide range of heavy particle sizes observed by Habibi (1971), one might expect that the broad spectrum of heavy particles should be subdivided into several size groups with appropriate settling velocities. However, Hage (1961) showed that the rate of deposition of particles in a turbulent flow may be obscured by non-uniformity of particle size. Further, it was shown by Van der Hoven (1968) that a vertical shear of the horizontal wind becomes as important as the diffusion mechanism if there were an initial variation of particle size with height. Habibi's wind tunnel tests (1973) showed that the heaviest particles had effective settling velocities between 0.06 and 0.25 m sec^{-1}. Considering the above factors, it was assumed that the heaviest particles could be represented by a single group with an effective settling velocity of 0.20 m sec^{-1}.

Habibi's studies also show that particles smaller than 10 μm were also deposited near the source in the wind tunnel. However, it should be noted that a particle with an effective aerodynamic diameter of 10 μm has a Stokes velocity of 0.3 cm sec^{-1} and a sub-micron particle of 0.2 μm has a Stokes velocity of 0.0123 cm sec^{-1}. For these highway studies, even under rather light wind conditions (a long travel time), a rather small amount of gravitational settling would have occurred for particles 10 μm and smaller. Particles in a size range from 0.5 to 10.0 μm are then probably being removed primarily by surface deposition, impaction or sorption. To describe this removal, an empirically determined, effective deposition velocity, v_d, of 0.01 m sec^{-1} was assigned to this class of particles.

In a previous modeling study (Reiter and Katen, 1972), it was shown that differences of concentration between gas-diffusion model predictions and particulate lead measurements reach about 35% within 60 m of the roadway. From a comparison of the measured and predicted fallout, it can be seen that gravitational settling and surface deposition do not fully account for the discrepancy between the earlier-model predictions and the measurements. One must conclude that the differences are not entirely attributable to the loss of particulate matter from the dispersing plume.

Apparently, other physical processes are important in the dispersion, and must be included in the diffusion equation. Based on the available data on particle sizes for highway driving conditions, and also considering the physical problem under study, the lead emissions were classified into the categories given in Table 5.1. The table gives the range of values observed in each group and also the average used in this study. These three categories classify the particulates as follows: a) the heaviest particles which undergo rapid gravitational settling, b) the intermediate-size particles which have a finite gravitational settling velocity, but are primarily removed by surface impaction or sorption at the surface, and c) the smallest, gas-like particles which are very slowly removed by surface interactions, and may be considered to be conserved during our observational periods.

iii. Parameterization of Vehicle Effects

A single vehicle moving along a roadway will create a wake which can be observed for several meters on either side of and above the vehicle after the vehicle has passed the observation point. The moving vehicle creates a region of low pressure of nearly its rear cross-section in the area directly behind the vehicle. Exhaust gases and particulates are usually released near the bottom of this low pressure region and are very vigorously drawn up into it. Turbulent inflowing air (with a Reynolds number >> 100,000) and the vehicle exhaust are quickly mixed. This single-vehicle release can then be advected and diffused by the boundary layer flow, and can be acted on by the turbulence from other vehicles. Dabberdt (1975) has shown that vehicle-generated turbulence on a heavily traveled (100,000 vehicles per day) divided highway creates a mixed layer of nearly uniform turbulence extending to about 4 m above the surface and 10 m beyond the traffic lanes. The vehicle-generated turbulence damps out quickly about 7.5 m above the surface. The effect of the traffic turbulence is to create some initial distribution of the pollutants over the roadway. In this model, the release is represented by two virtual line sources lying in the middle of each side of the divided roadway, at a height of 1.6 m.

TABLE 5.1

Percentage by weight of lead consumed by vehicles. Range of observations and average values used in this study.

SIZE	DESCRIPTION OF PARTICLE BEHAVIOR	OVERALL RANGE	AVERAGE
---	Retained in Vehicle	10-90%	30%
$d < 0.5$ µm	Gas-Like	5-50%	25%
0.5 µm $< d <$ 10 µm	Surface Deposition	5-40%	35%
$d > 10$ µm	Gravitational Settling	5-20%	10%
		TOTAL	100%

The small-scale vehicle turbulence is parameterized as an effective eddy diffusivity, K_v, which is superimposed on the eddy diffusivity of the surface layer given by Eq. 2.20. This effective eddy diffusivity was assumed to be constant throughout the field with a value of 0.5 $m^2 sec^{-1}$. In his study of the diffusion of carbon monoxide from a highway, Danard (1972) assumed an eddy diffusivity of 20 $m^2 sec^{-1}$ in the lowest 3 m over the highway. This value was assumed to decrease linearly with distance, to the value of the atmospheric eddy diffusivitity at 50 m from the edge of the roadway. In our study, a vehicle turbulence decay rate was not assumed. The approach taken was to assume that the net effect of the vehicle turbulence on the dispersion was limited (based on an average of the observations) to a maximum contribution to the plume variance (σ_z^2) of 50 m^2. The effect of the vehicle turbulence is (usually) initially greater than that of the atmospheric turbulence near the roadway in the lowest layers. At greater distances from the roadway, the dispersion becomes dependent on atmospheric turbulence alone, since the vehicle eddy diffusivity was assumed to be of limited strength.

A detailed analysis of the measured distributions, discussed in the following sections, indicates that a factor in addition to mechanical turbulence (atmospheric and vehicular) was acting to disperse the lead particulates. It was found that the dispersing plume had an effective vertical displacement and it is necessary to give a buoyant velocity, v_b, of 0.15 m sec^{-1} to the plume to improve the agreement between the model predictions and the measurements.

Several mechanisms are thought to contribute to this plume behavior. Thermal emissions from the vehicles are partly responsible for the large cross-roadway temperature gradients observed by Dabberdt (1975), who shows that the exhaust heat released on a heavily traveled roadway can be a significant percentage of the solar radiation falling on the roadway. Furthermore, Dabberdt (1976) has suggested that a line of vehicles on a roadway may act as a "shelter-belt" effect, which would have the effect of slightly decreasing the mean wind speed in the region just downwind of the roadway. One would also expect to find a trailing vortex shed from the lee side of the vehicles as they move along the roadway. Since in our study the traffic densities were considerably less than those studied by Dabberdt, the vehicular waste heat emissions are probably not intense enough, by themselves, to give the exhaust plume a significant buoyancy. However, it is felt that the combined effects of vehicle-generated turbulence, waste heat and, in some cases, an unstable surface layer, can act together to trigger this buoyant plume. The result is that the dispersing plume attains a net upward vertical wind component. From the observations, it appears that this induced vertical motion is of limited intensity and in agreement with the measurements, the plume centerline was allowed to rise a maximum of 8.0 m above the effective source height.

C. A Model For the Dispersion of Lead from a Highway

i. The Highway Dispersion Model

A general form of the diffusion equation which combines both the vehicular effects and atmospheric profiles is given by

$$u(z)\frac{\partial c}{\partial x} + (v_b + v_g)\frac{\partial c}{\partial z} = \frac{\partial}{\partial z}(K_z(z) + K_v)\frac{\partial c}{\partial z} \quad (5.1)$$

where $u(z)$ is the measured atmospheric wind profile, v_b the buoyant velocity of the exhaust plume, v_g the gravitational settling velocity of the lead bearing particulates, $K_z(z)$ the eddy diffusivity of the surface layer given by Eq. 2.20, and K_v the eddy diffusivity attributable to vehicle movement. If one assumes that conditions are homogeneous so that u, $v_b + v_g$, and $K_z + K_v$ are all constants, the solution to Eq. 5.1 is given from the basic homogeneous (or Gaussian) solutions discussed in Chapter 2.

The homogeneous solution to Eq. 5.1 is given by

$$c = \frac{Q_L'}{\sqrt{2\pi}\sqrt{2K_z t + 2K_v t}\;u}\exp\left\{-\frac{1}{2}\frac{(z-h-(v_b+v_g)t)^2}{(2K_z t + 2K_v t)}\right\} +$$

$$\exp\left\{\frac{1}{2}\frac{(z+h+(v_b+v_g)t)^2}{(2K_z t + 2K_v t)}\right\} \quad (5.2a)$$

$$\text{where} \quad Q_L' = Q_L\left[\exp\left\{-\frac{v_d \times c(x,0)}{Q_L}\right\}\right] \quad , \quad (5.2b)$$

h is the height of the virtual source above the surface, and t is the downwind travel time from the virtual source to the receptor point. This specific homogeneous solution can be used to approximate the numerical solution of Eq. 5.1 for inhomogeneous conditions with the use of the modified Gaussian solution technique described in Chapter 3.

Equation 5.2 has been written to encompass the dispersion of all three sizes of lead particles from a highway. The three homogeneous solutions for the size groups given in Table 5.1 can be obtained from Eq. 5.2 by various assumptions on v_b and v_d: a) for the large particles undergoing gravitational settling, v_g = -0.2 m sec^{-1} and $v_d = 0$; b) for the intermediate size particles $v_g = 0$ and v_d = 0.01 m sec^{-1}; and c) for the smallest particles $v_g = v_d = 0$.

The initial source strength, Q_L, for each particle size theoretically can be determined from: a) the percentage of the consumed lead in the size range given in Table 5.1; b) an assumed average of 2.0 gms of lead per gallon of gasoline; c) an average vehicle mileage of 13 miles per gallon; and d) the number of vehicles per hour passing the test site. However, it was necessary to determine the effective source strengths given in Table 5.2 from a comparison of measured and predicted concentrations by initially establishing an effective number of vehicles with a, b and c above held constant.

The plume variance is determined as the sum of the variance due to atmospheric turbulence and vehicle turbulence and is given by

$$\sigma_z^2 = 2K_v t + 2K_z(z)t \tag{5.3}$$

where $K_v = 0.5\ m^2sec^{-1}$, K_z is given by Eq. 2.20, and $t = x/u(z)$. Both $K_z(z)$ and $u(z)$ are the effective values as evaluated in Appendix A. The first term on the right-hand side of Eq. 5.3 is limited to a maximum value of $50.0\ m^2$.

This highway model does not incorporate any effect of the eddies generated by south-bound traffic on the dispersion of the north-bound lane emissions. Dabberdt (1975) has shown that the ratio of σ_z (north-bound lanes) to σ_z (south-bound lanes) at comparable dispersion distance, varies from 0.3 to 3.0; the ratio had the highest correlation with wind speed alone, of all the parameters tested. Since no clear systematic relationship was established, in this study, the growth of the up-wind and down-wind lanes were assumed to be independent.

TABLE 5.2

Source strength determined from the effective number of vehicles per hour (VPH), its intensity (μg of lead $m^{-1}sec^{-1}$) and the mass remaining in the profile at 48 m (μg of lead $m^{-1}sec^{-1}$).

Figure	Test/Run	Effective VPH	Source Strength	Mass in Profile at 48 m
5.2a	4	1200	23.8	20.6
5.2b	5-1	2276	43.3	37.1
5.2c	5-2	1500	26.2	22.6
5.2d	7	1116	20.7	16.8
5.2e	8-1	792	14.7	12.4
5.2f	8-2	1000	18.6	15.0
5.2g	10	1860	34.6	28.5

ii. Analysis of the Data

Seven data sets are presented for comparison with the highway model formulated in the previous section. The model predictions were used to establish the maxima of K_v and v_b. The measured profiles of u, σ_w and T_E are given in Figs. 5.1a to 5.1g. Table 5.3 gives the statistics of the boundary layer which were used with the data in Fig. 4.10 and Eq. 2.20 to calculate the atmospheric profiles of eddy diffusivity.

Figures 5.2a to 5.2g display isopleths of atmospheric lead concentrations in a plane perpendicular to the highway. The horizontal distance, x, is the distance from the downwind edge of the pavement. (The virtual sources are at x = -6.4 m and x = -33.8 m.) The height, z, is height from the surface. Each of these x-z cross-sections (Figs. 5.2a to 5.2g) contains the values of the measured concentrations at the locations indicated by the dots. In addition, each cross-section contains two sets of predictions. Those marked in heavy lines are predicted with the complete highway model described in the previous section. Those isopleths marked with the dashed lines were predicted by the same model, but with $v_b = K_v = 0$.

One can best understand the effects of the vehicles on the dispersion by comparing the predictions with and without the parameterized vehicle effects. There are two very noticeable characteristics in the measured concentration patterns given in Figs. 5.2. They are the small vertical concentration gradient along the tower at 48 m and the small horizontal concentration gradients downwind of this tower (x = 48 m).

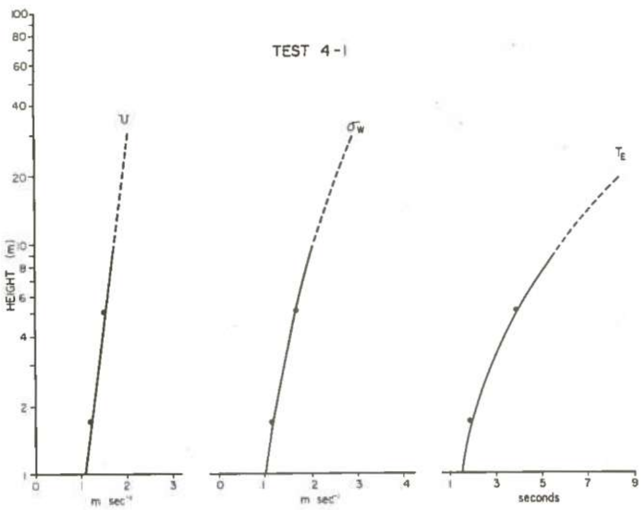

Figure 5.1a. Measured boundary layer profiles of wind speed, u, vertical wind standard deviation, σ_w, and Euerian integral time scale, T_E for the highway lead dispersion study, Test 4-1.

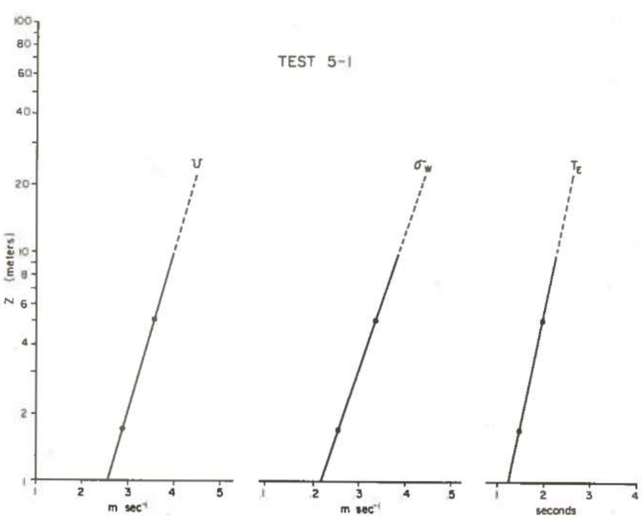

Figure 5.1b. Same as Fig. 5.1a except for Test 5-1.

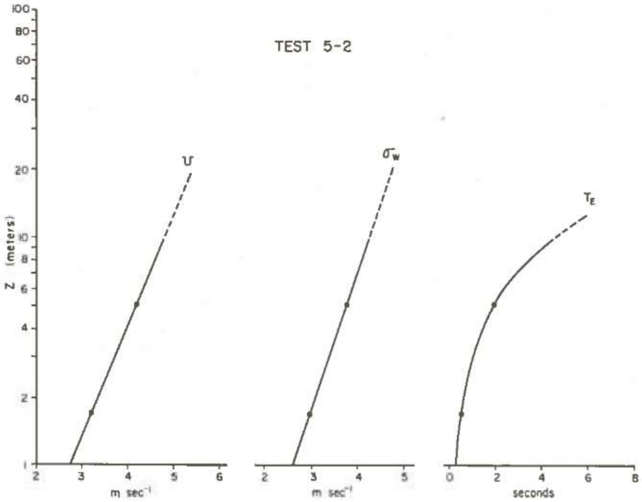

Figure 5.1c. Same as Fig. 5.1a except for Test 5.2.

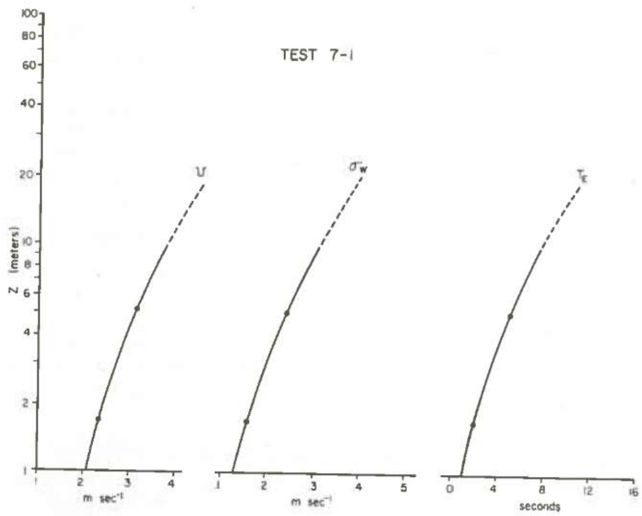

Figure 5.1d. Same as Fig. 5.1a except for Test 7-1.

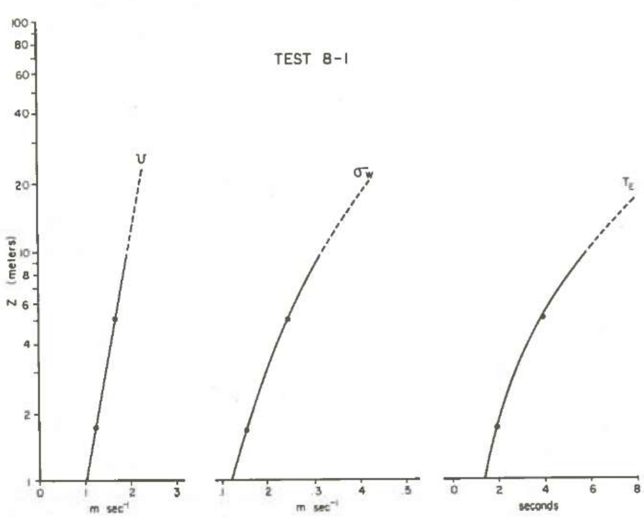

Figure 5.1e. Same as Fig. 5.1a except for Test 8-1.

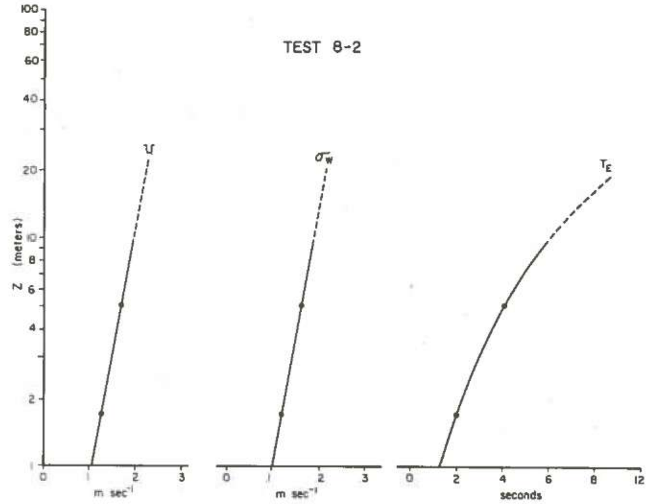

Figure 5.1f. Same as Fig. 5.1a except for Test 8-2.

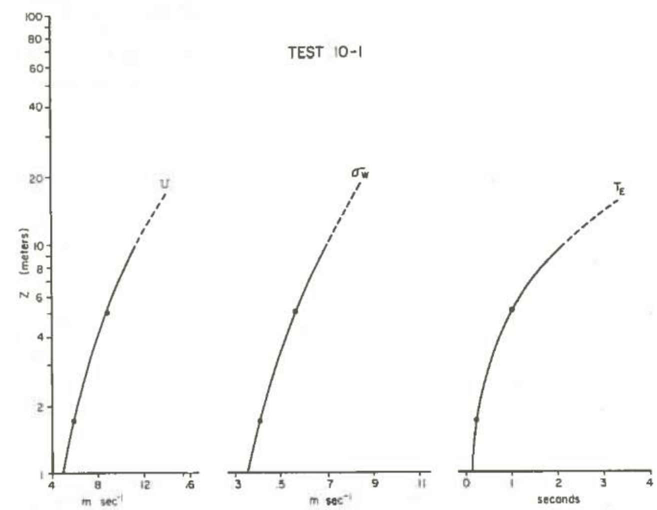

Figure 5.1g. Same as Fig. 5.1a except for Test 10-1.

TABLE 5.3

Highway test data. Here ϕ is the angle of the wind with respect to the normal to the roadway, u_* the friction velocity, z_0 the roughness length, and L the Monin-Obukhov length.

DATE	TEST	ϕ	u_*(m sec^{-1})	z_0(cm)	L(m)
8/17/71	4	24°	0.11	1.4	- 10.24
8/17/71	5-1	24°	0.50	9.0	- 19.07
8/17/71	5-2	24°	0.52	11.7	- 24.95
9/24/71	7	65°	0.38	32	- 21.72
9/27/71	8-1	18°	0.33	16	- 2.80
9/27/71	8-2	61°	0.26	15	- 7.63
10/07/71	10	57°	1.08	17	-402.2

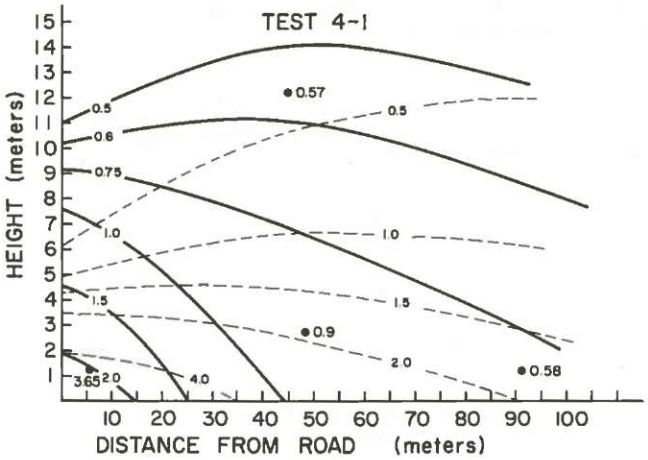

Figure 5.2a. Predicted isopleths of lead concentration, in micrograms per cubic meter, in a plane perpendicular to the highway for Test 4-1. Dashed lines are values predicted by atmospheric turbulence alone, and solid lines are dispersion patterns predicted for the combined atmospheric and vehicular effects. Measured concentrations were sampled at the locations indicated by the dots.

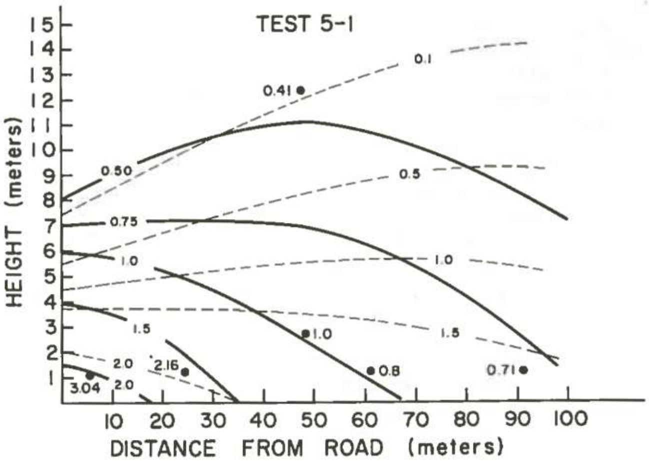

Figure 5.2b. Same as Fig. 5.2a except for Test 5-1.

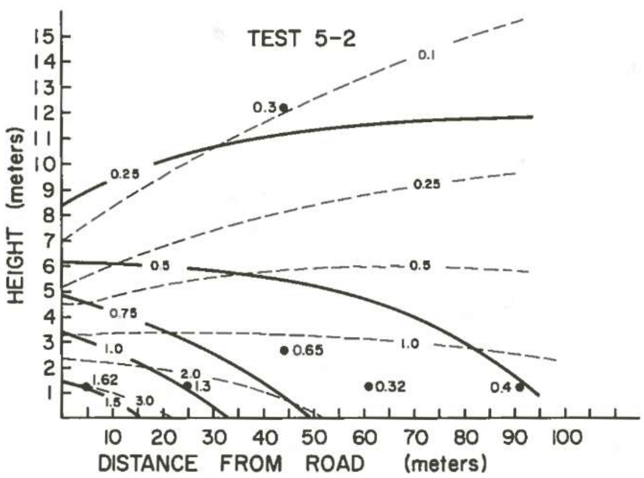

Figure 5.2c. Same as Fig. 5.2a except for Test 5-2.

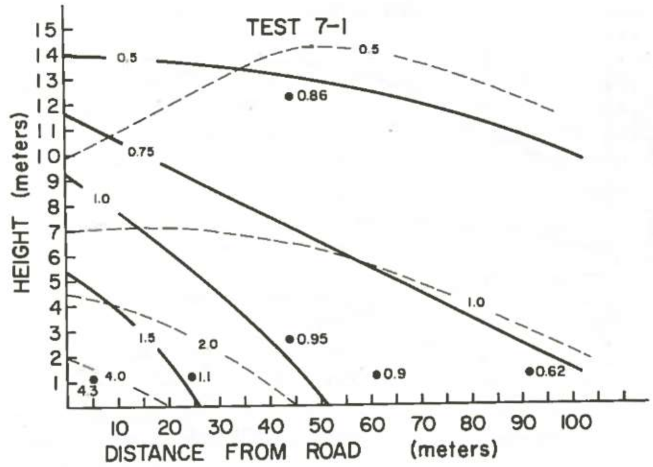

Figure 5.2d. Same as Figure 5.2a except for Test 7-1.

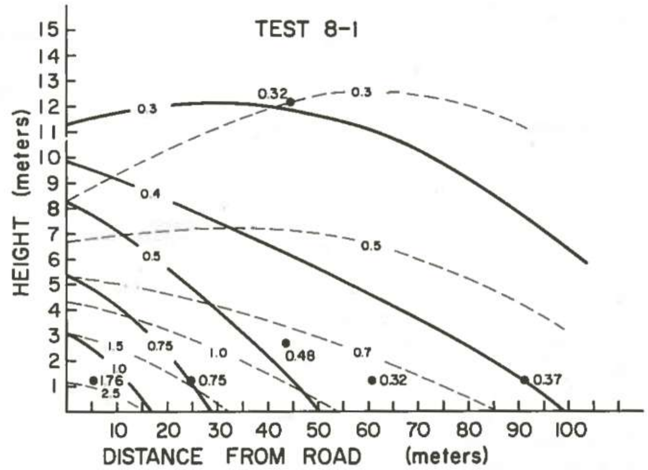

Figure 5.2e. Same as Fig. 5.2a except for Test 8-1.

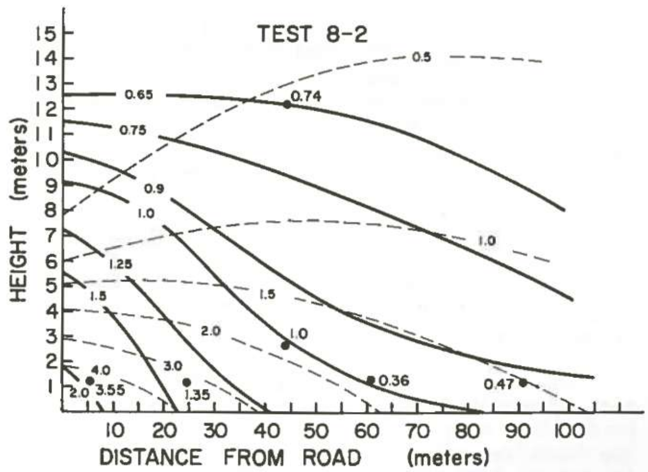

Figure 5.2f. Same as Fig. 5.2a except for Test 8-2.

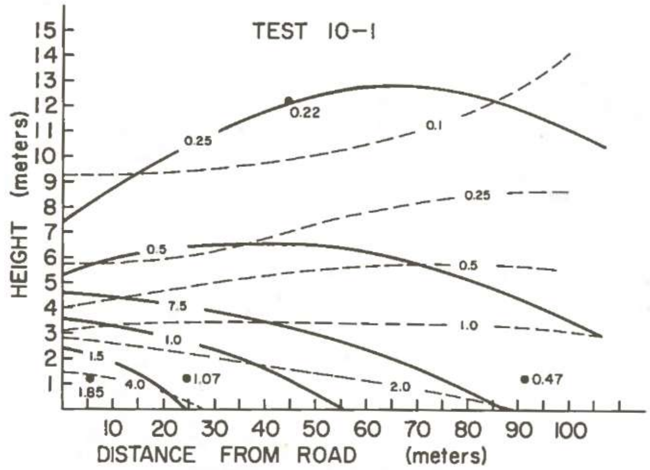

Figure 5.2g. Same as Fig. 5.2a except for Test 10-1.

From Figs. 5.2a to 5.2g one can see that the measured concentration gradients in these regions are about one-half to one-fourth of the gradients predicted when atmospheric eddy diffusivity alone is used in the evaluation. Inclusion of K_v and v_b leads to the agreement of the highway model predictions and the measurements. One exception to this is Fig. 5.2f, Test 8-2. In this case the differences are due to errors in the measurements.

Another noticable characteristic of the predicted patterns is the increased vertical spread near the pavement, x = 0. The greatest vertical plume spread at the roadside occurs in Figs. 5.2d, Test 7-1 and 5.2f, Test 8-2. In these cases, from Figs. 5.1d and 5.1f the wind speeds are quite low, as seen in a travel time (calculated at a height of 3 m) from the resulting farthest virtual source (x = -33.8) to the reference plane (x = 0) of approximately 45 seconds. This long travel time allows the dispersing plume from the north-bound lanes to attain this large vertical spread by the time it reaches the road edge. The farthest lanes upwind contribute greater than 95% of the mass to receptor points above 9 m at the road edge. In these two test cases, it should also be noted that the dispersion predicted by atmospheric turbulence alone shows also a rather broad distribution at the downwind road edge.

The model which includes vehicle turbulence does not, in all cases, yield good predictions near the roadway (the first sampler is at x = 5.2 m). This is due to the fact that this first sampler is actually in a different flow regime. This regime is part of the "well mixed" layer discussed by Dabberdt (1975), which was observed to extend 10 m beyond the traffic region. To correctly model this region near the roadway, it is necessary to assume that the flow field variables, u and K_z, are functions of x as well as z in that region. However, detailed information on the structure of the flow field in and around the traffic lanes is not now available.

The data presented in Figs. 5.2a and 5.2e, show good agreement between the measurements and the model predictions except for rather large disagreements at the roadside sampler, x = 5.2m. In these two cases the travel time from the reference plane, x = 0, to the main tower, x = 48 m, is approximately 35 sec. These examples illustrate the basic inadequacy of the model when the vehicle effects are much stronger than those of the atmosphere in the turbulent region near the roadway.

There are some test conditions under which this highway model does show good agreement at all the measuring locations. The best overall agreement occurs in Figs. 5.2c and 5.2g. In these cases, the wind is strong and the travel time from the roadside to the main tower, x = 48 m, is about 13 seconds (calculated at a height of 3 m). In these cases, atmospheric eddy diffusivity was quite large. The effects of the atmospheric processes are as strong as the vehicle effects. The plume, in the region of study, can be seen to be undergoing rapid growth with downwind travel.

After a travel time of approximately 50 seconds from the virtual line sources, K_z and v_b become ineffective. This indicates that atmospheric eddy diffusivity eventually becomes the primary mechanism in the dispersion. This transition to an unperturbed turbulent regime is demonstrated in Figs. 5.2a to 5.2g. The transition can be considered to begin when the two sets of isopleths in each diagram tend toward similar patterns. In several of the cases, e.g., Figs. 5.2d,e,f the transition begins at about x = 50.0 m. Thus it is necessary to include the vehicular effects only in the region immediately adjacent to the roadway.

Table 5.3 also presents the data on the mass of lead still remaining in the predicted profile at 48 m. The mass of lead remaining in the profile at 48 m is an indication of the depletion of the plume by the removal processes. This decrease is due to both a loss of heavy particles by gravitational settling and a loss of intermediately-sized particles by surface deposition.

iii. Summary

The generally good agreement of the predictions of this model with measurements is encouraging. Hence, the dispersion of lead from a roadway can be described with the model suggested in this chapter. The model, however, has certain limitations. It does not make accurate predictions close to the traffic lanes when the atmospheric eddy diffusivity is small compared to the eddy diffusivity attributable to the vehicle-generated turbulence.

The best agreement with the measurements occurs when the Monin-Obukhov length, L, is less than -25 m, a condition under which the mechanical generation of turbulent kinetic energy dominates over the buoyant production. Under these conditions the atmospheric turbulence in the boundary layer usually equals or exceeds the vehicle turbulence for moderately traveled highways.

Far (x > 50m) from the roadway the vehicle effects become secondary to atmospheric turbulence. This is observed as a trend towards the alignment of the two sets of isopleths predicted with and without vehicle effects. At greater distances from the highway, one can completely neglect the initial influence of the vehicles on the dispersion.

The data given in Table 5.3 indicate that only about 10% of the consumed lead, or 15% of the emitted lead, is lost from the plume by gravitational settling and surface removal over the range of this study. From this one can conclude that a large vertical plume spread and not surface deposition is responsible for the rapid decrease of concentration with increasing distance from the highway.

6. Conclusions and Recommendations

A. Conclusions

Simple analytical solutions exist for homogeneous diffusion equations. However, atmospheric flow fields are often inhomogeneous and are governed by inhomogeneous diffusion equations, for which no general analytical solutions exist. On the other hand, numerical solutions consume considerable computational time, even with moderately large computer facilities. Thus, there is a need to find accurate, general and easily computable methods to solve inhomogeneous diffusion equations.

It is shown that the effective values of the mean wind and eddy diffusivity can be introduced into the Gaussian solution of a homogeneous diffusion equation to yield a useful solution for the inhomogeneous case. The technique is called the method of modified Gaussian solution. In many of our experiments, the measured and predicted distributions are in close agreement.

The method of modified Gaussian solution is applied to the diffusion of gases and particulate matter from line sources such as highways. The predictions of this method agree with those of the numerical method including such characteristics as the general shape of the distribution, the downward displacement of maximum concentration, and the upward displacement of the center of gravity of the plume.

The gas-diffusion studies show that two-dimensional K theory describes the diffusion sufficiently well. A comparison of three techniques for formulating eddy diffusivity shows that Taylor's theory and similarity theory do not yield acceptable coefficients of diffusion, and that the long-diffusion time, asymptotic limit to Taylor's theory yields the best results.

The application of the method of modified Gaussian solution and the parameterized eddy diffusivity to the study of the highway dispersion of lead shows that while some particulate lead is lost from the dispersing plume, the rapid decrease in concentration with distance from the roadway is primarily due to vertical transport.

The vertical spread of the plume cannot be accounted for by the measured atmospheric turbulence alone. While the anemometers do not measure the very small, vehicle-generated eddies, the concentration profiles show their effect.

The following quantities were included in the model to describe the observed concentration profiles: a) a buoyancy of the plume and b) an effective eddy diffusivity. This eddy diffusivity is due to the vehicle-generated turbulence and the buoyancy, in part, arises from heated exhaust gases. The vehicle turbulence initially contributes significantly to the dispersion but its energy is rapidly dissipated. At greater distances from the roadway, dispersion is dominated by the atmospheric processes alone.

B. Suggestions for Future Research

More accurate methods need to be devised to parameterize the effective values of the flow-field variables for the method of modified Gaussian solution. A study should be made as to whether the method can be extended to inhomogeneities in all three dimensions.

The factor β', used in the scaling of the Eulerian measurements in the formulation of the eddy diffusivity was assumed to be a constant throughout the surface layer. But this may not be true. More detailed study is necessary to determine any variations of β' with height and the dependency of it on the non-dimensional height $z/|L|$.

Gaseous tracer studies should be conducted in the region immediately adjacent to the roadway to investigate the buoyancy effect and eddy diffusivity attributable to the vehicles in greater detail. These studies should establish both the dependency of these quantities on vehicle density and their decay rates as a function of distance from the roadway.

References

Abramowitz, M. and I.A. Stegun, 1968: Handbook of Mathematical functions. Dover Publications, Inc., 1046 pp.

Baldwin, L.W. and W.R. Mickelson, 1963: Turbulent Diffusion and Anemometer Measurements. Trans. ASCE, 128 Part I, 1595-1631.

Bezner, I.D. and P.R. Atkins, 1970: The Dispersion of Lead and Carbon Monoxide from a Heavily Traveled Highway. Technical Report EHE-70-08, Dept. of Civil Engineering, Univ. of Texas at Austin, Austin, Texas.

Brier, G.W., 1961: Some Statistical Aspects of Long-Term Fluctuations in Solar and Atmospheric Phenomena. Annals of the New York Academy of Sciences, 95, 173-187.

Businger, J.A., 1972: The Atmospheric Boundary Layer. Remote Sensing of the Troposphere, Ch. 6, Wave Propagation Laboratory, Boulder, Colorado.

Calder, K.L., 1973: On Estimating Air Pollution Concentration from a Highway in an Oblique Wind. Atmospheric Environment, 7, 863-868.

Clemons, C.A., A.I. Coleman and B.E. Saltzman, 1968: Concentration and Ultrasensitive Chromatographic Determination of Sulfur Hexafluoride for Applications to Meteorological Tracing. Envir. Sci. and Tech., 7, 551-556.

Corrin, M.L., 1971: Atmospheric Chemistry. Impact on Man of Environmental Contamination Caused by Lead. H.W. Edwards, ed., Interim Report, Dept. Mechanical Engineering, Colorado State University, Ft. Collins, Colo.

_____, and M. Menne, 1975: Personal Communication.

Corrsin, S., 1963: Estimation of the Relation Between Eulerian and Lagrangian Scale in Large Reynolds Number Turbulence. J. Atmos. Sci., 20, 115-119.

_____, 1974: Limitations of Gradient Transport Models in Random Walks and in Turbulence. Turbulent Diffusion in Environmental Pollution, F.N. Frankiel and R.E. Munn, eds., Advances in Geophysics, 18A, Academic Press, London, pp. 462.

Cotton, W., 1975: Personal Communication.

Csanady, G.T., 1974: Turbulent Diffusion in the Envionment. D. Reidel Publishing Co., 248 pp.

_____, G.R. Hilst and N.E. Bowne, 1968: Turbulent Diffusion from a Cross-Wind Line Source in Shear Flow at Fort Wayne, Indiana. Atmos. Envir., 2, 273-292.

Dabberdt, W.F., 1975: Multiple-Tracer Highway Dispersion Study. SRI, Menlo Park, Calif., Presented at International Conference on Environmental Sensing and Assessment, Sept. 14-19, 1975, Las Vegas, Nevada.

_____, 1976: Experimental Studies of Near-Roadway Dispersion. Presented at 69th Annual Meeting of the APCA, June 27 - July 1, 1976, Portland, Oregon.

Dannard, M.B., 1972: Numerical Modeling of Carbon Monoxide Concentrations Near Highways. J. Appl. Met., 11, 947-957.

Drivas, P.J. and F.H. Shair, 1974: Dispersion of an Instantaneous Cross-Wind Line Source of Tracer Released from an Urban Highway. Atmos. Envir., 8, 475-485.

Dyer, A.J., 1974: A Review of Flux-Profile Relationships. Bound. Layer Met., 7, 363-372.

Edwards, H.W., ed., 1971: Impact on Man of Environmental Contamination Caused by Lead. Interim Report, Dept. Mechanical Engineering, Colo. State Univ., Fort Collins, Colo.

_____, 1972: Impact on Man of Environmental Contamination Caused by Lead. Interim Report, Dept. Mechanical Engineering, Colo. State Univ., Fort Collins, Colorado.

_____, 1973. Impact on Man of Environmental Contamination Caused by Lead. Interim Report, Dept. Mechanical Engineering, Colo. State Univ., Fort Collins, Colorado.

_____, 1974. Impact on Man of Environmental Contamination Caused by Lead. Interim Report, Dept. Mechanical Engineering, Colo. State Univ., Fort Collins, Colo.

Fuchs, N., 1964: The Mechanics of Aerosols. Macmillian and Co., New York, 168 pp.

Habibi, K., 1970: Characterization of Particulate Lead in Vehicle Exhaust - Experimental Techniques. Envir. Sci. and Tech., 4, 239-248.

_____, 1973: Characterization of Particulate Lead in Vehicle Exhaust. Envir. Sci. and Tech., 7, 223-234.

_____, K.S. Jacobs, W.G. Kunz, Jr. and D.L. Pastell, 1970: Characterization and Control of Gaseous and Particulate Exhaust Emissions from Vehicles. Presented at APCA, West Coast Section - Fifth Technical Meeting, Oct. 8-9, 1970, San Francisco, Calif.

Hage, K.D., 1961: The Influence of Size Distribution on the Ground Deposition of Large Particles Emitted from an Elevated Source. Int. J. Air and Water Poll., 4, 24-32.

Hay, J.S. and F. Pasquill, 1957: Diffusion from a Continuous Source in Relation to the Spectrum and Scale of Turbulence. F.N. Frankiel and P.A. Sheapard, eds., Advances in Geophysics, 6, p. 245, Academic Press.

Hinze, J.O., 1959: Turbulence. McGraw Hill Book Co., 586 pp.

Hirschler, D.A., L.F. Gilbert, F.W. Lamb and L.M. Niebylski, 1957: Particulate Lead Compounds in Automobile Exhaust Gas. Industrial and Engineering Chemistry, 49, 1131-1142.

Horst, T.W., 1973: Corrections for Response Errors in a Three-Component Propeller Anemometer. J. Appl. Met., 12, 716-725.

Lumley, J.L., 1962: The Mathematical Nature of the Problem Relating Lagrangian and Eulerian Statistical Functions in Turbulence. In: Mecanique de La Turbulence, Ed. du Centre Nat. de la Rech. Sci., Paris, pp. 17-26.

_____, and H.A. Panofsky, 1964: The Structure of Atmospheric Turbulence. Interscience Publishers, 239 pp.

Lutz, G.A., A.A. Levin, S.G. Bloom, K.L. Nielson, J.L. Cross and D.L. Morrison, 1970: Final Report, Vol. III. Lead Model Case Study. U.S. Dept. Health, Educ. and Welfare, Contract #CPS-69-005, Battelle Memorial Institute, Columbus, Ohio.

Mielke, P., 1972: Personal Communication.

Monin, A.S. and A.M. Obukhov, 1954: Basic Laws of Turbulent Mixing in the Ground Layer of the Atmosphere. Akad. Nauk. SSSR. Geofiz. Inst. Trudy, 151, 163-187.

Pasquill, F., 1962: Atmospheric Diffusion. D. Van Nostrand Co., Ltd., 297 pp.

Reiter, E.R. and P.C. Katen, 1972: Atmospheric Transport of Lead. Impact on Man of Environmental Contamination Caused by Lead. H.W. Edwards, ed., Interim Report, Dept. Mechanical Engineering, Colo. State Univ., Fort Collins, Colo.

Richtmyer, R.D., and K.W. Morton, 1967: Difference Methods for Initial Valve Problems. Interscience Publishers, 405 pp.

Robinson, E. and F.L. Ludwig, 1967: Particle Size Distribution of Urban Lead Aerosols. J. Air Poll. Control Assoc., 17, 664-668.

Rounds, W., Jr., 1955: Solution of the Two-Dimensional Diffusion Equations; Transactions. AGU, 36(2), 395-405.

Slade, D.H., ed., 1968: Meteorology and Atomic Energy 1968. Atomic Energy Commission, TID-24190, 445 pp.

Sutton, O.G., 1953: Micrometeorology. McGraw Hill, 333 pp.

Taylor, G.I., 1921: Diffusion by Continuous Movements. Proc. London Math. Soc. (2), 20, 196-212.

Ter Haar, G.L., D.L. Lenane, J.N. Hu and M. Brandt, 1972: Composition, Size and Control of Automotive Exhaust Particulates. J. Air Poll. Control Assoc., 22, 39-46.

Turk, A., S.M. Edmonds and H.L. Mark, 1968: Sulfur Hexafluoride as a Gas Tracer. Envir. Sci. and Tech., 2, 44-48.

Turner, B.D., 1964: Workbook of Atmospheric Dispersion Estimates. EPA, Research Triangle Park, N.C.

Van Buijtenen, C.J.P., J. Holland and D. Van Leeuwen, 1972: A Numerical Diffusion Model for Continuous Releases. Bound. Layer Met., 5, 275-283.

Van Der Hoven, I., 1968: Deposition of Particles and Gases. Meteorology and Atomic Energy 1968, D.H. Slade, ed., Atomic Energy Commission, TID-24190, pp. 202-208.

Walters, T.S., 1957: Diffusion from an Infinite Line Source Lying Perpendicular to the Mean Wind Velocity of a Turbulent Flow. Quart. J. Mech. and Appl. Math., X, pt. 2, 214-219.

Zimdahl, R.L., 1972: Lead in Soils and Plants. Impact on Man of Environmental Contamination Caused by Lead, H.W. Edwards, ed., Dept. Mechanical Engineering, Colo. State Univ., Fort Collins, Colo., pp. 98-123.

Appendix A

Determination of the "Effective Field of Influence"

The object of this appendix is to present the empirical method used in this study for estimating the effective field of influence at a given receptor point. The formulae given here were determined experimentally from a comparison of solutions by the method of modified Gaussian solution and numerical finite difference or analytical solutions to the governing differential equations. These formulae are proved to be adequate in most of the cases studied. However, it is felt that improvements will be made on the technique in the future.

In determining the effective field of influence it is necessary to establish a) whether the plume has grown wide enough so as to have had significant interaction with the surface and b) whether the receptor point is closer to the peak of the distribution or closer to the tail of the distribution. This is done by comparing both the reference (source) height of the plume, z_{ref}, and the difference in elevation between the source and receptor heights, $z_{rel}\left(=\left|z_{ref}-z_r\right|\right)$, with a parameter σ_{geo}, where σ_{geo} is a factor representative of the dispersive capabilities of the region between the source height and the surface. The factor σ_{geo} is given by

$$\sigma_{geo} = \sqrt{2\, K_{geo}\, x/u_{geo}}$$

where K_{geo} and u_{geo} are the geometric averages of $K(z)$ and $u(z)$ over the region from the surface (in actuality the lowest grid level) to the source level and x is the distance downstream of the source.

Vertical grid spacings for these calculations were determined primarily on mass continuity considerations given by

$$Q_L = \int_0^\infty c(x,z)u(z)dz.$$

Calculations with different vertical grid spacings showed that the grid spacing in the vertical direction is not critical to the prediction of the concentration distribution. Uniform vertical grid spacings varying from 0.1 to 3.0 m have been tested successfully on plumes with various degrees of spread. In the examples presented in this dissertation, 0.2 m is used in most of the cases. Near the source, where concentration gradients are steep, Δz must be small, whereas at greater distance downwind, Δz can be quite large.

Two empirical scaling lengths used in defining the extent of the effective field of influence are given by

$$A = 0.818\, \sigma_{ref}$$

and

$$B = 0.818\, \sigma_{ref}\, (\sigma_r/\sigma_{ref})$$

where $\sigma_{ref} = \sqrt{2\, K_{ref}\, x/u_{ref}}$, $\sigma_r = \sqrt{2\, K_r\, x/u_r}$, K_{ref} and K_r, u_{ref} and u_r are the values of eddy diffusivity and wind speed at the source and receptor levels, respectively.

A. Elevated Line Source

Two general cases are distinguished depending on whether the plume centerline is "near" or "far" from the surface.

A) Source Level Located <u>Far</u> From the Surface ($z_{ref} > 1.95\, \sigma_{geo}$). <u>In</u> this case the proximity of the receptor point to the plume centerline must also be established.

1) If the receptor point is within a distance of 1.5 σ_{geo} of the source level, then the effective field of influence encompasses the region enclosed by the source level and the receptor level plus a distance <u>A</u> above and below the region.

2) If the receptor point is greater than a distance of 1.5 σ_{geo} from the source level (case 1 in Fig. A-1), then the averaging region encompasses the region enclosed by the two levels and extends a distance <u>A</u> above (below) the source level and a distance <u>B</u> below (above) the receptor level when the receptor is below (above) the source level.

B) Source Level Located <u>Near</u> The Surface ($z_{ref} \le 1.95\, \sigma_{geo}$). <u>In</u> this case (given as Case-2 in Fig. A-1) the averaging begins at the lowest z level and extends to a height given by

$$z = z_{ref} + z_r + 2\sigma_{geo}.$$

B. Line Source Near the Surface

A special case is when the source is at the surface, or for practical considerations, at the lowest grid level. In this case the effective field of influence should begin at the source level (lowest grid level) and extend to the height given by

$$z = z_{ref} + z_r + 4A.$$

From the example discussed in Chapter 3, it seems that the effective field of influence probably should not extend to the receptor point when the receptor point is far into the tail of the distribution. This indicates that the upper regions of the field do not influence the distribution as strongly as the lower regions, and the effective field of influence must be adjusted so as not to give the same weighting to the upper region as to the lower region.

C. Calculation of the Effective Values

Once the effective fields of influence for the field variables u and K_z are determined, geometric averages for each are calculated over that region. These geometric averages are then used to evaluate the Gaussian solution to determine the concentration at that receptor point. This process must be repeated for each receptor point to determine the entire concentration distribution.

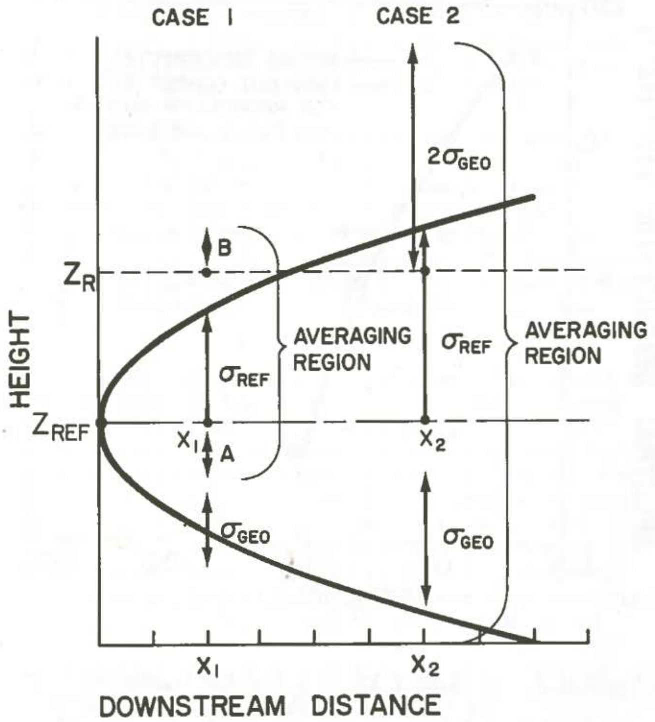

Figure A.1. A schematic representation of the regions over which the field variables u and K_z must be averaged to determine the effective values of those field variables for the receptor level z_r. Arrows indicate approximate magnitudes of the parameters σ_{ref}, σ_{geo}, A and B at the downwind distances x_1 and x_2. Case 1: the source is "far" from the surface and the receptor point is greater than 1.5 times the distance σ_{geo} from the source level. Case 2: the source level is "near" the surface.

APPENDIX B

Field Equipment and Data Processing

Two field programs were conducted in association with the dispersion studies discussed in this dissertation. The first was a study of the vertical diffusion of a gas (SF_6) from a cross-wind line source. The second was a study of the short-range, atmospheric dispersion of lead particulates from a highway. The purpose of this appendix is to discuss the details of the equipment used in these two studies. This will include the design of hardware and the use and calibration of analytical equipment.

A. Sulfur Hexafluoride Dispersion Studies

The physical configuration for this dispersion study is given in Figs. 4.1, 4.2 and 4.3. In order to complete this program it was necessary to design, build, calibrate and deploy each component used in this study. These systems included: a line source, a sampling system, and SF_6 and meteorological systems.

i. Bivane Anemometers

The bivane anemometers used were manufactured by the R.M. Young Company, Model Number 21002. The measuring unit consists of A) a propellor and a wind vane capable of measuring the speed, and azimuthal and elevation angles of the instanteous wind vector, and B) the translational unit which powers the direction vane and processes the signal for output to a recording instrument.

The instantaneous position of the bivane is mechanically translated to slide-wire resistors, which are powered by a 28-volt power supply. Position of the vane is indicated by an output voltage and is related to the mechanical position of the vane through a prior mechanical-electrical calibration. The anemometer consisted of a four-bladed, 7 1/2 inch propellor to drive a DC generator and four-finned tail capable of responding to both lateral and vertical wind fluctuations. The manufacturer's test data shows that the threshold wind of the propellor/generator unit is 0.5 m sec^{-1}, and that the propellor and vane, which are closely matched in dynamic response characteristics, have an amplitude ratio of about 63% for a gust length of 4 m. To define the vertical profile of the mean and turbulent wind fields, four bivane anemometers were mounted on the main sampling tower at heights of 1.5, 3.1, 7.5, and 18.5 m.

ii. Bivane Anemometer Corrections

Unfortunately, at present there are no data in the literature concerning the accuracy of these bivanes. To be assured that the characteristics quoted by the manufacturer truly represented the response of the bivane to each of the three variables being measured (viz., speed, azimuth and elevation angle), bivane anemometer statistics were compared to those of a Gill UVW anemometer (R.M. Young Co., Model 27002). In a recent study Horst (1973) compared the UVW anemometer and a sonic anemometer, which he considered to be "an appropriate standard". This comparison showed that with a correction for the non-cosine response of the propellors to a wind not parallel to the propellor axis and a correction for propellor inertia, most statistics of the two anemometors agreed within a few percent. In addition, the data presented by Horst showed a good correlation of the spectral response of his two test instruments. For purposes of comparison, in our studies, the UVW anemometer was considered to be the standard against which the bivane anemometer frequency spectra were to be compared. The primary, but not exclusive, source of data was an experiment conducted on June 7, 1974, when the anemometers were deployed in the following way: Three bivanes and one UVW anemometer were placed at a sensing height of 1.5 m from the ground and one bivane and one UVW anemometer were placed at a sensing height of 3.1 m. Data was collected and digitally recorded continually for a period of 5.5 hours, from which three one-half hour periods were selected for detailed analysis. The sample digitizing rate was approximately 25 channels per sec, and the spectrum analysis was limited to a maximum frequency of 1.10 Hz. The spectra discussed in this section were calculated by Fourier-transforming the velocity autocorrelation coefficient as discussed by Pasquill (1962).

In Fig. B.1, curves A and B give the manufacturer's dynamic response of the vane and propellor as a function of wavelength. Curve C gives the dynamic response of the system (the product of curves A and

B). Based on this information, only a small correction factor would have to be applied, above a wavelength of 8 m, to correct for the physical and inertial filtering characteristics of the anemometer. From this one would expect the measurements to slightly underestimate the variance of the wind.

The energy spectra of the u-component is shown in Fig. B.2. In this figure, curve A is the measured (uncorrected) energy spectrum of the bivane. It compares very well with curve B, the spectrum for the UVW anemometer, which is corrected for non-cosine response as discussed by Horst, but not for propellor inertia. The propellors used on the bivane and UVW anemometers have nearly identical dynamic characteristics. If one uses the frequency response correction factor derived by Horst to correct both curves for propellor inertia, the agreement between the two curves is still excellent. For clarity, only the corrected curve for the UVW anemometer is shown (curve C). These results indicate that the bivane measures the u component fluctuations well.

The energy spectra shown in Fig. B.3, are for the vertical components, for both types of anemometers. Curve A is for the UVW which is corrected for non-cosine response only. Curve B is for the UVW with corrections for non-cosine response and propellor inertia. Curve C is for the w components of the bivane. When compared to the curve for the UVW, one can see that the bivane has a very dramatic over-response. In all cases studied, the measured, uncorrected, w component bivane spectra, had a sharp break in its slope; also, it crossed the UVW spectra. If one converts the abscissa of Fig. B.3 from frequency to gust wavelength (which equals wind speed divided by frequency), the two critical points in curve C occur at significant wavelengths. The cross-over point of the UVW and bivane spectra occurs at nearly 4.5 m and the sharp break seen in all the bivane spectra occurs at nearly 9.0 m. These wavelengths are the theoretical undamped natural wavelength of the vane (as quoted by the manufacturer) and twice the theoretical undamped natural wavelength, respectively. Further, at wavelengths less than 4.5 m the bivane spectrum is severely attenuated, since the

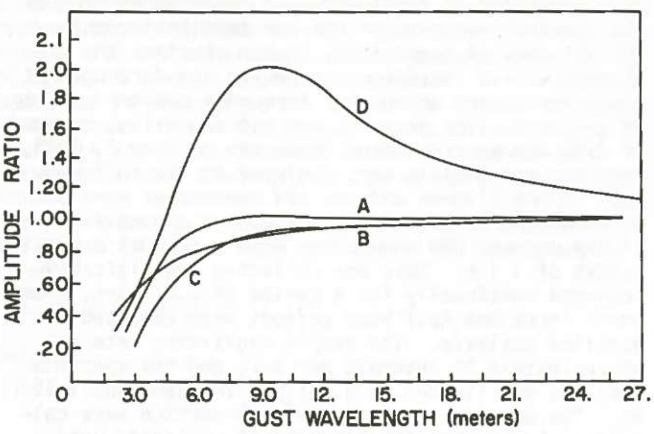

Figure B.1. The response characteristic of the bivane anemometer. Curves A and B are for the vane and propellor, respectively, as given in curve C, which is the product of A and B. Curve D is the response of the system to the vertical wind as measured in this study.

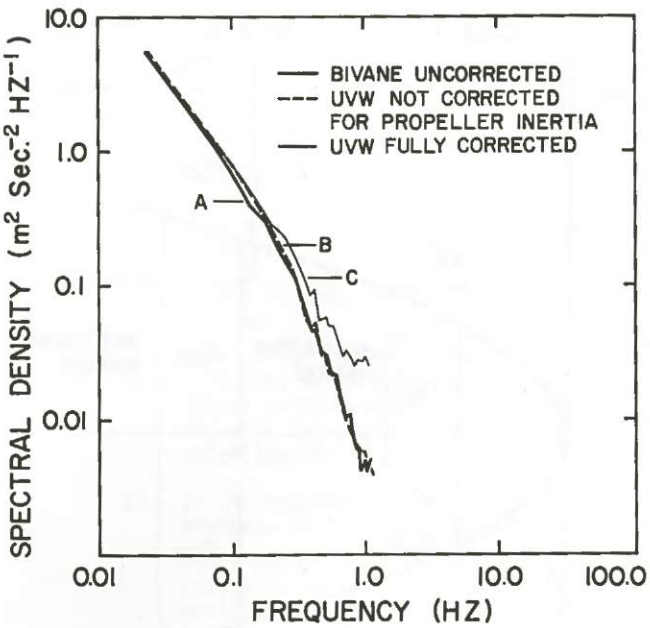

Figure B.2. Frequency spectra for the u component of the bivane and UVW anemometers. Curve A is the uncorrected curve for the bivane. Curve B is with a correction for non-cosine response and curve C is with a correction for non-cosine response plus a correction for propellor inertia.

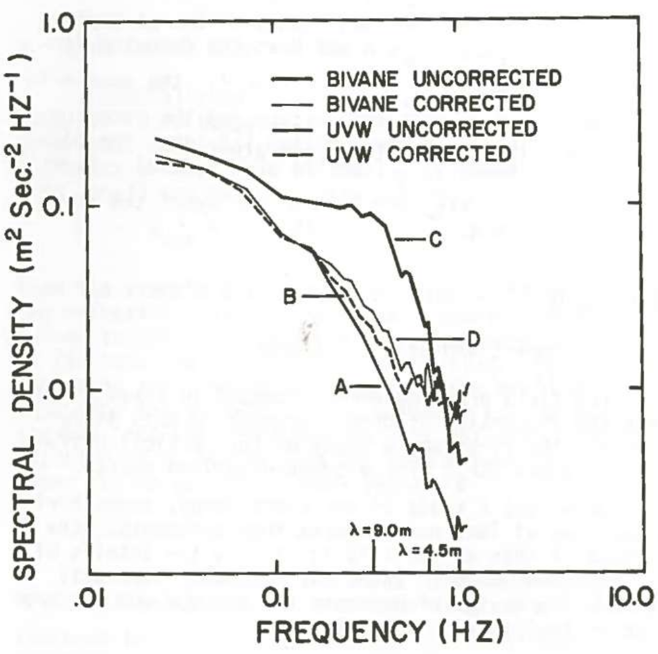

Figure B.3. Energy spectra for the w-component of the bivane and UVW anemometers. Curve A is the uncorrected UVW, curve B is the fully corrected UVW, Curve C is the uncorrected bivane, and curve D is the corrected bivane.

vane inadequately responds to these short waves. Beyond about 10 times the theoretical undamped natural wavelength, there is a rather constant over-response of 10% (in the range of frequencies studied).

There are several approaches one may use to correct for this over-response. To further use the original time series, which was used to generate this spectrum, one could design a filtering function to remove this observed bias from the original time series (Brier, 1961). In that case, the uncorrected individual observations would be used in conjunction with a weighting function to generate a new time series.

In this study, we are interested in obtaining a true estimate of the variance of the vertical wind component from the bivane measurements. For this reason it was only necessary to derive an empirical, wavelength-dependent weighting function, as the one shown in Fig. B.4. This weighting function is then used to correct the bivane spectra to agree with that of the UVW. (A simpler approach would have been to scale the variance empirically, but this would not have resulted in an explanation of the over-response.) The result of using the weighting function on the measured (uncorrected) bivane spectrum is given in Table B.1 and Fig. B.3, curve D, as the corrected bivane values. Figure B.3 shows that the corrected bivane and corrected UVW anemometers are in good agreement. The UVW anemometer data in Table B.1 is corrected as suggested by Horst (1973). This table shows that the bivane corrections are quite significant.

The implications of this weighting function (Fig. B.4) are better understood if it is converted into a dynamic response curve for the bivane. The square root of the inverse of this weighting function (Fig. B.4) is plotted as curve D in Fig. B.1. This shows that the behavior, in the vertical of the bivane, is quite different from that given by the manufacturer. Apparently, some factors have been overlooked in the design of this instrument. While other vane anemometers are capable of accurately resolving the two horizontal wind components, u and v, the relatively small variances of the w component, near the surface ($< 0.1\ m^2 sec^{-2}$) are easily overestimated with the bivane. It appears that the vertical swings of the vane translate too large a fraction of the horizontal wind components into the vertical component.

Since reasonable agreement between the w-spectra of the bivane anemometers and the UVW anemometers is achieved by introducing a weighting function in the case of the bivane, this weighting function will be applied to correct for instrumental errors.

iii. Temperature Measurement

The surface layer temperature profile measuring system consisted of 4 shielded thermocouples mounted at heights of 0.5, 1.5, 7.5, and 11.0 m. The thermocouples were of copper-constantan and were read out on a Doric Model Number DS-100-T3, temperature-compensated, digital thermometer. The thermocouple junction was calibrated for each test with an ice bath. The readout and wire system were found to be within manufacturer's stated accuracy of $\underset{\sim}{\sim}$ 0.05°C. However, it was found that under variable ambient conditions the temperature-compensating unit varied by as much as 0.3°C on warm days, but under these conditions all thermocouples still agree within $\pm$ 0.05°C. Thus, while the absolute accuracy of the unit varied, its

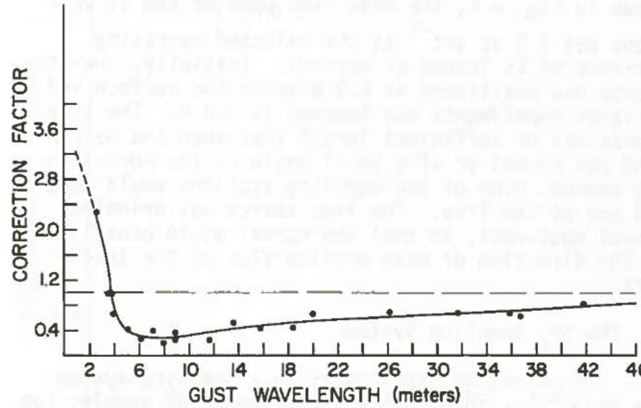

Figure B.4. Empirical correction factor applied to the w-component spectra of the bivane anemometers to correct for the observed over-response.

TABLE B.1

Bivane and UVW anemometer vertical wind component statistics

	σ	σ^2
Corrected UVW	0.180	0.0326
Uncorrected Bivane	0.252	0.0635
Corrected Bivane	0.174	0.0303

relative accuracy remained constant. This was felt sufficient for the intended purposes of measuring vertical temperature gradients although not for absolute temperature profiles.

iv. Line Source

The line source was 60 m long and was constructed in the following manner: one inch segments of 0.012 inch inside diameter (ID) hypodermic tubing were mounted in a silicone plug in the "T" leg of a 3/8 inch brass Polyflo tubing connector (Polyflo is the trade name for Imperial-Eastman polyethylene tubing). Sections of 3/8 inch Polyflo tubing were cut, so that when connected with the "T" fitting the hypodermic tubes would be separated by 2 m. The use of 3/8 inch outside diameter (OD; 1/4 inch ID) tubing insured that the manifold static pressure would be uniform throughout, resulting in a uniform metering of SF_6 along the full length of the line source. The center of the line source was connected to a feed line from a bottle of 99.9% pure SF_6. Pressure in the feed line/manifold system was monitored with a mercury manometer.

The source tubes were cut from hypodermic tubing stock with the ends being deburred and quality of each tube checked before use. Before assembling the line source, each section of hypodermic tubing was flow-calibrated over the full range of operating pressures using a 100 cc bubble flow meter. Once the line source was assembled and positioned for the field program, each of the 31 orifices were re-checked and verified to be clear and operating correctly. As shown in Fig. B.5, the mean flow rate of the 31 orifices was 9.6 cc sec^{-1} at the selected operating pressure of 24 inches of mercury. Initially, the line source was positioned at 6.5 m above the surface and in later experiments was lowered to 2.8 m. The line source was of sufficient length that when the mean wind was normal or at a small angle to the normal to the source, none of the sampling stations would "see" the end of the line. The line source was oriented almost east-west, so that the normal would usually be in the direction of mean daytime flow at the test site.

v. The SF_6 Sampling System

The object in fabricating this sampling system was to be able to obtain a large number of samples (up to 32 simultaneously) for each test release, and integrate them over sampling periods of up to 30 minutes. The sampling system was designed to operate efficiently using a minimum of resources.

Three sampling towers were used for the collection of samples. The first tower, 8.7 m in height, was 16.5 m downwind from the line source and had seven sampling locations each separated by one meter (see Fig. 4.2). The second tower, 18.3 m tall and 31.0 m from the source had up to 15 possible sampling ports. Most had a separation of 1 m, but a few were more closely spaced near the release height for better delineation of concentration patterns in this critical region. A third tower 11.4 m tall and 45.5 m from the line source had 10 sampling ports each separated by one meter. The polyethylene sampling tubes were firmly attached to a rope with the vertical spacings discussed above. The rope was in turn suspended from a boom which protruded 0.6 m out from the towers. It was then possible to move the sampling manifold up and down on each tower, anywhere from the surface to several meters above the surface, to coincide with various release heights (Fig. B.6a). The sampling tubes were then connected to the sampling container at the surface. All sampling tubes had a minimum length of 12.5 m with a maximum of 21.0 m. This was done so that once sampling began, all bags received a minimum volume of 175 and a maximum of 290 cc of clear air. The tubing had a volume of $\sim$ 14 cc m^{-1}. Measured concentrations were then adjusted to compensate for this dilution as discussed below. Sampling bags were mounted inside of sealed steel containers and were connected to the sampling lines outside with a bulkhead fitting (Fig. B.6b). Earlier studies, which used sulfur hexaflouride as a tracer (Clemons, et al., 1968), showed that Saran bags are the best material for collection and storage. To accurately control the sampling rate each bulkhead fitting was sealed with a silicone plug and a 2.5 cm section of 0.020 inch ID hypodermic tubing was inserted through the plug as shown in Fig. B.6c. The sampling rate could be further regulated by adjusting the degree of vacuum within the container, which was measured with a water manometer. Tests were conducted so that the five 1/2-liter Saran bags would be filled to about 3/4 of capacity in 25 minutes of sampling.

vi. Gas Chromatography for SF_6 Measurements

Concentration profiles for the SF_6 releases were analyzed with a Hewlett Packard Model 7620A Research Gas Chromatograph (GC). The technique used was essentially that described by Turk et al. (1968). The SF_6 was separated from the air with the use of silica gel and activated charcoal columns in series. The SF_6

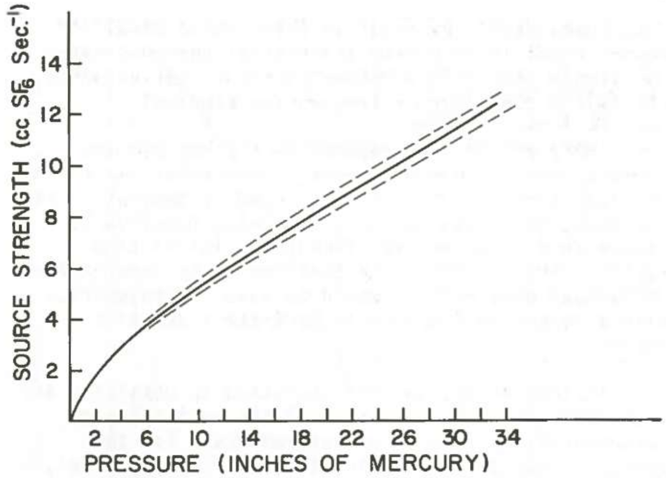

Figure B.5. Mean flow rate of SF_6 from the 31 sections hypodermic tubing used in fabricating the line source for the airport study. Dashed lines show the range of values in the calibration data.

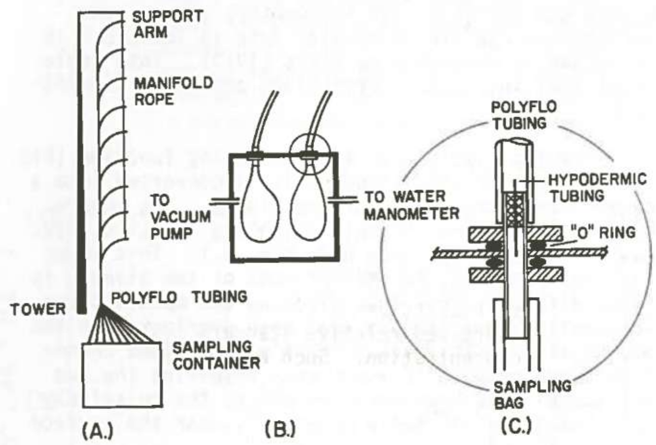

Figure B.6. Representation of sampling system for measurement of SF_6 concentration profiles.

Figure A shows the tower, sampling lines and collecting container; Figure B shows detail of collecting container; and Figure C shows a detail of bulkhead fitting with silicone plug and hypodermic tubing.

was detected with a pulsed electron capture detector using a tritium source. The major difference between this approach and that of Turk et al. was that they used 1 m columns of both silica gel and activated charcoal, but here adequate separation of the various air and SF_6 peaks could be obtained with 1/2-m columns, at a column flow rate of 20 cc per minute. The output signals from the GC were electronically integrated to give the peak area.

The calibration technique was designed to help establish the slope of the linear response curve typical of the electron capture detector. This technique, which was cross-checked with a certified standard, was also shown to have both good accuracy and precision. To calibrate the chromatograph over the full range of operating conditions it was necessary to formulate additional calibration standards. These were generated in a sequential dilution process and extended the calibration curve considerably below 1 ppb (parts per billion).

Several 1-liter reagent bottles (thoroughly cleansed and baked) were fitted with a one-hole rubber stopper through which a glass tube was inserted and capped with a bottle septum. The total volume of each bottle system was determined with water. A typical dilution sequence is as follows: 1 cc of pure SF_6 was injected into a bottle yielding a concentration of 832 ppm. One cubic centimeter of this mixture (after adequate mixing time) was injected into a second bottle yielding a concentration of 731 ppb; one further dilution gave a standard of 0.64 ppb. An example of a calibration curve is given in Fig. B.7. This figure includes data from several dilution sequences as well as from the certified standard. The linear curve was determined by a least squares fit, with the origin included as a data point.

To be assured that the dilution technique was not introducing any cumulative errors due to adsorption, an independent test was conducted. Four standards were formulated, two each had two dilutions and two others each had three dilutions. If cumulative losses were occurring, two differently sloped curves would have resulted. However, all four points were found to lie on the same line.

To determine the precision of the laboratory procedure, ten injections were made of each of three standards, 13.1, 63.2 and 183 ppb. The analysis showed that each of the sets of ten injections had standard deviations of 0.42, 1.53, and 1.58 ppb, yielding relative standard deviations of 3.2, 2.4, and 0.86%. These results demonstrated the anticipated results of increased relative standard deviation with decreasing concentration. Such a trend arises since instrumental errors become proportionally larger at the lower concentrations. The use of Pressure-Lok Syringes manufactured by the Precision Sampling Company was in part responsible for the good precision obtained in this analysis.

vii. Measured Profile Corrections

The uncertainties in the precision of the gas chormatograph calibration and the sample dilution from the tubing and bag dead volumes lead to errors in the absolute values of the SF_6 concentrations. The extent of these errors can be determined by an independent test. A conservation of mass test can establish the amount of gas accounted for by the measured concentration profile and is given by

$$Q_M = \eta \int_0^z c(x, z)\, u(z)\, dz, \qquad (4.1)$$

where Q_M is the measured source strength, η is the concentration profile factor (initially assumed as $\eta = 1$). By comparing the known release source strength, Q_L, to the measured source strength, Q_M, one can then scale the measured profile by the appropriate value ($\eta = Q_L/Q_M$) to correct for measurement errors. The errors due to sample dilution were such that the measured profiles accounted for about 75-80% of the gas which was being released.

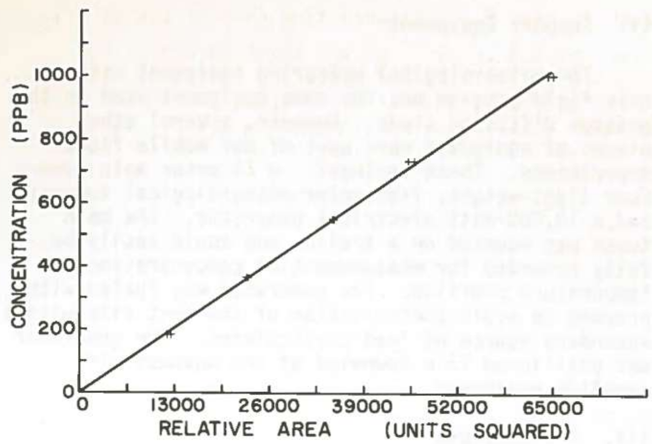

Figure B.7. Example of a gas chromatograph calibration curve determined by using both the certified standard and standards generated by the sequential dilution process.

B. Particulate Lead Dispersion Studies

i. Equipment Deployment at the Highway Test Site

In designing the field program the first air sampler was placed, as conveniently and safely as possible, at the downwind edge of the nearest travel lane. The four lowest-level samplers were placed at a mean height of 1.2 m with the 20.3 x 25.4 cm filter holder extending from about 1.1 m to 1.3 m above the actual surface. The four lowest samplers were placed at the following distances from the roadway: 5.2, 24.5, 62.0, and 92.0 m. In addition, two samplers were mounted on the tower, located 48.0 m from the downwind edge of the roadway, at heights of 2.7 m and 12.2 m. These were used to define the diffusing plume's vertical characteristics. While the terrain was not perfectly flat, the slight elevation variations were neglected. None of the terrain features were sufficiently serious to perturb the air flow. All height measurements were made with respect to the local surface. The net elevation variation from the roadway to the last sampler, at 92 m from the roadway, was about 0.5 m. The range of the study approximately 100 m from the roadway, was determined to be the maximum anticipated distance from the roadway for which the filter background lead blank would not exceed 5% of the total lead which could be collected in a 30-minute sampling period.

In this field program, four bivane anemometers were used to study the mean and turbulent wind field. Two were placed in a vertical column 62.0 m from the roadway at heights of 1.7 and 5.0 m. The other two bivanes were also placed at 5.0 m, one at a distance of 24.5 m and the other at 92.0 m from the roadway. The object of placing three anemometers in a horizontal plane 5 m above the surface was to look at longitudinal variations in the wind field as might be caused by the traffic. However, no longitudinal inhomogeneity was measured. It is felt that vehicle-generated turbulence is of sufficiently small scale that the bivanes with a response wavelength of the order of 4 m could not detect it.

ii. Support Equipment

The meteorological measuring equipment used in this field program was the same equipment used in the gaseous diffusion study. However, several other pieces of equipment were part of our mobile field experiments. These included: a 15 meter main tower; four light-weight, five meter meteorological towers; and a 10,000 watt electrical generator. The main tower was mounted on a trailer and could easily be fully extended for measurement of concentration and temperature profiles. The generator was fueled with propane to avoid contamination of the test site with a secondary source of lead particulates. The generator was positioned 25 m downwind of the nearest air sampling equipment.

iii. Air Samplers

During the early stages of the lead study an air sampling technique was developed for measuring airborne lead-bearing particulates using a high-volume air sampler (Corrin, 1971). The technique used a Gelman Hurricane (high volume) air sampler and a 20.3 x 25.4 cm filter holder. The filtering medium consisted of a triacetate Metricel filter with a 5-μm pore size. This metrical filter was backed by a fiberglass, type A filter paper, which isolated it from the holder and blower. Field studies conducted by Corrin (1971) showed the efficiency of this filter for lead-bearing particulates, to be as good as the standard type A and comparable to that of 0.01 μm Metricel filters. The amount of lead contained in an unused 20.3 x 24.5 cm 5 μm filter was approximately 1.5 μg (Corrin, 1971). Thus an accuracy of 5% could be obtained for samples containing 30 μg of lead, typical of those collected near roadways in 30 minutes.

In order to calculate the atmospheric concentration of particulate lead it was necessary to know accurately the total volume of air passed through the filter as well as the mass of lead collected. The high-volume air sampler has a flow-metering device included in the unit. Calibration of these units indicated that severe errors could occur due to the design of the measuring units. A second measuring device was used to make all flow measurements. Since the typical flow rate was about 1 m^3 min^{-1} of air through the filter, but only at a static pressure of 5 cm (gauge) of water, it was thus necessary to use a high-volume, low-resistance, flow-measuring device. The instrument used was the Laminar Flow Device Model Number 50 MC2-25, manufactured by the Meriam Instrument Company.

The results of this independent flow calibration indicated that the flow-measuring devices built into the high-volume samplers were generally in error from 15% to 45%.

iv. Filter Analysis

Filter analysis was accomplished as follows: Filters were cut into quarters and each section was dissolved in 10 cc of 3 molar nitric acid. Samples were aspirated into the burner of a Varian-Techtron AA5 atomic absorption spectrophotometer. For this analysis, the instrument was equipped with a standard hollow cathode Pb 208 lamp and the monochromator set at the 2170 Å lead line. The degree of attenuation of the signal beam with respect to the reference beam was an indication of the concentration of lead in the test solution. Calibration was accomplished through a series of standard solutions, and background was corrected for with an H_2 hollow cathode lamp. Instrumental parameters were optimized near the values suggested by the manufacturer to improve the signal-to-noise ratio. These factors included: lamp current, fuel/air ratios for flame stoichiometry, nebulizer flow rate and burner position.

statistical theory nor similarity theory yields an appropriate eddy diffusivity. An empirical formula, based on the asymptotic form of Taylor's theory, yields the best results.

A model is then designed, using the method of modified Gaussian solution, for predicting the atmospheric dispersion of particulate lead from a highway. The highway dispersion model employs the results of the gas-diffusion experiments to clarify the role of vehicle-generated turbulence in the dispersion process. The vehicle effects are included as an eddy diffusivity attributable to the moving vehicles and as a buoyancy caused by exhaust heat from the vehicles. The vehicle-generated turbulence and buoyancy are shown to be important in the dispersion process up to about 50 m from the roadway. Thereafter, dispersion is dominated by atmospheric turbulence. A large upward plume spread -- and not the loss of material by deposition -- is primarily responsible for the observed, rapid decrease in concentration with increasing distance from the highway.

statistical theory nor similarity theory yields an appropriate eddy diffusivity. An empirical formula, based on the asymptotic form of Taylor's theory, yields the best results.

A model is then designed, using the method of modified Gaussian solution, for predicting the atmospheric dispersion of particulate lead from a highway. The highway dispersion model employs the results of the gas-diffusion experiments to clarify the role of vehicle-generated turbulence in the dispersion process. The vehicle effects are included as an eddy diffusivity attributable to the moving vehicles and as a buoyancy caused by exhaust heat from the vehicles. The vehicle-generated turbulence and buoyancy are shown to be important in the dispersion process up to about 50 m from the roadway. Thereafter, dispersion is dominated by atmospheric turbulence. A large upward plume spread -- and not the loss of material by deposition -- is primarily responsible for the observed, rapid decrease in concentration with increasing distance from the highway.

statistical theory nor similarity theory yields an appropriate eddy diffusivity. An empirical formula, based on the asymptotic form of Taylor's theory, yields the best results.

A model is then designed, using the method of modified Gaussian solution, for predicting the atmospheric dispersion of particulate lead from a highway. The highway dispersion model employs the results of the gas-diffusion experiments to clarify the role of vehicle-generated turbulence in the dispersion process. The vehicle effects are included as an eddy diffusivity attributable to the moving vehicles and as a buoyancy caused by exhaust heat from the vehicles. The vehicle-generated turbulence and buoyancy are shown to be important in the dispersion process up to about 50 m from the roadway. Thereafter, dispersion is dominated by atmospheric turbulence. A large upward plume spread -- and not the loss of material by deposition -- is primarily responsible for the observed, rapid decrease in concentration with increasing distance from the highway.

statistical theory nor similarity theory yields an appropriate eddy diffusivity. An empirical formula, based on the asymptotic form of Taylor's theory, yields the best results.

A model is then designed, using the method of modified Gaussian solution, for predicting the atmospheric dispersion of particulate lead from a highway. The highway dispersion model employs the results of the gas-diffusion experiments to clarify the role of vehicle-generated turbulence in the dispersion process. The vehicle effects are included as an eddy diffusivity attributable to the moving vehicles and as a buoyancy caused by exhaust heat from the vehicles. The vehicle-generated turbulence and buoyancy are shown to be important in the dispersion process up to about 50 m from the roadway. Thereafter, dispersion is dominated by atmospheric turbulence. A large upward plume spread -- and not the loss of material by deposition -- is primarily responsible for the observed, rapid decrease in concentration with increasing distance from the highway.

Author: Paul C. Katen 551.511.6

MODELING ATMOSPHERIC DISPERSION OF
LEAD PARTICULATES FROM A HIGHWAY

Colorado State University
Department of Atmospheric Science

Environmental Research Paper No. 11
October 1977. 36 pp.

National Science Foundation
Grant Nos. GI-44423 and AEN-74-17624-A01
Energy Research and Development Administration

Subject Headings:

Theoretical Background
The Method of Modified Gaussain Solution
Line Source Gas-Diffusion Experiments
Modeling the Dispersion of Lead Particulates From a Highway

In this report we develop a method which will predict the diffusion of lead-bearing particulates emitted by vehicles moving on a highway. The method of modified Gaussian solution, developed through analogy with finite-differencing techniques, when applied to a diffusion equation, fulfills this purpose. This solution meets our demands of accuracy and ease of computation.

It is shown that Gaussian solutions can be applied to the diffusion of gases and particulates emanating from line sources, such as a highway.

We try to establish, through an experimental study, the best method of formulating eddy diffusivity for the short-range dispersion of gaseous pollutants from a line source. This study shows that neither Taylor's

Author: Paul C. Katen 551.511.6

MODELING ATMOSPHERIC DISPERSION OF
LEAD PARTICULATES FROM A HIGHWAY

Colorado State University
Department of Atmospheric Science

Environmental Research Paper No. 11
October 1977. 36 pp.

National Science Foundation
Grant Nos. GI-44423 and AEN-74-17624-A01
Energy Research and Development Administration

Subject Headings:

Theoretical Background
The Method of Modified Gaussain Solution
Line Source Gas-Diffusion Experiments
Modeling the Dispersion of Lead Particulates From a Highway

In this report we develop a method which will predict the diffusion of lead-bearing particulates emitted by vehicles moving on a highway. The method of modified Gaussian solution, developed through analogy with finite-differencing techniques, when applied to a diffusion equation, fulfills this purpose. This solution meets our demands of accuracy and ease of computation.

It is shown that Gaussian solutions can be applied to the diffusion of gases and particulates emanating from line sources, such as a highway.

We try to establish, through an experimental study, the best method of formulating eddy diffusivity for the short-range dispersion of gaseous pollutants from a line source. This study shows that neither Taylor's

Author: Paul C. Katen 551.511.6

MODELING ATMOSPHERIC DISPERSION OF
LEAD PARTICULATES FROM A HIGHWAY

Colorado State University
Department of Atmospheric Science

Environmental Research Paper No. 11
October 1977. 36 pp.

National Science Foundation
Grant Nos. GI-44423 and AEN-74-17624-A01
Energy Research and Development Administration

Subject Headings:

Theoretical Background
The Method of Modified Gaussain Solution
Line Source Gas-Diffusion Experiments
Modeling the Dispersion of Lead Particulates From a Highway

In this report we develop a method which will predict the diffusion of lead-bearing particulates emitted by vehicles moving on a highway. The method of modified Gaussian solution, developed through analogy with finite-differencing techniques, when applied to a diffusion equation, fulfills this purpose. This solution meets our demands of accuracy and ease of computation.

It is shown that Gaussian solutions can be applied to the diffusion of gases and particulates emanating from line sources, such as a highway.

We try to establish, through an experimental study, the best method of formulating eddy diffusivity for the short-range dispersion of gaseous pollutants from a line source. This study shows that neither Taylor's

Author: Paul C. Katen 551.511.6

MODELING ATMOSPHERIC DISPERSION OF
LEAD PARTICULATES FROM A HIGHWAY

Colorado State University
Department of Atmospheric Science

Environmental Research Paper No. 11
October 1977. 36 pp.

National Science Foundation
Grant Nos. GI-44423 and AEN-74-17624-A01
Energy Research and Development Administration

Subject Headings:

Theoretical Background
The Method of Modified Gaussain Solution
Line Source Gas-Diffusion Experiments
Modeling the Dispersion of Lead Particulates From a Highway

In this report we develop a method which will predict the diffusion of lead-bearing particulates emitted by vehicles moving on a highway. The method of modified Gaussian solution, developed through analogy with finite-differencing techniques, when applied to a diffusion equation, fulfills this purpose. This solution meets our demands of accuracy and ease of computation.

It is shown that Gaussian solutions can be applied to the diffusion of gases and particulates emanating from line sources, such as a highway.

We try to establish, through an experimental study, the best method of formulating eddy diffusivity for the short-range dispersion of gaseous pollutants from a line source. This study shows that neither Taylor's

Previously Published Environmental Research Papers

No. 1 On the Variability of Hemispheric Scale Energy Parameters, by J.P. McGuirk, E.R. Reiter and A.M. Barbieri, January 1975.

No. 2 On Determining Vertical Wind Velocities from Eole Constant-Density Balloon Data, by Robert M. Banta, June 1975.

No. 3 Atmospheric Eddy Transports and Their Efficiencies, by Srinivasan Srivatsangam, January 1976.

No. 4 Interannual Variations and Regional Effects of Hemispheric Parameters, by Ann M. Starr (neé Barbieri), July 1976.

No. 5 The Effects of Atmospheric Variability on Energy Utilization and Conservation, by E.R. Reiter et al., November 1976.

No. 6 Fluctuations in the Atmosphere's Energy Cycle, by James P. McGuirk, March 1977.

No. 7 Oceanic Latent and Sensible Heat Flux Variability and Air-Interaction, by Anne D. Seigel, April 1977.

No. 8 Observations of Stratospheric Thermal Structure from Satellites, by Thomas J. Kleespies, May 1977.

No. 9 Effects of Coal Mine Drainage on Macroinvertebrates of Trout Creek, Colorado, by Steven P. Canton and James V. Ward, April 1977.

No. 10 Potential Effects of Oil Shale Extraction and Processing Activities on Macroinvertebrates of Piceance and Black Sulphur Creeks, Colorado, by Lawrence J. Gray and James V. Ward, April 1977.